Measuring particle energy

Giovanni De Lellis
University Federico II and INFN Naples, Italy
NUST MISiS, Moscow, Russia

Giovanni.de.lellis@cern.ch

Calorimetry in Particle Physics

This lecture draws heavily from the Review Article
'Calorimetry for Particle Physics',
C.W. Fabjan and F. Gianotti, Rev. Mod. Phys., Vol. 75, NO. 4, October 2003

Much information was also taken from the massive Monograph

'Calorimetry, Energy Measurement in Particle Physics',
R. Wigmans, Oxford University Press, Second edition, 2017

Training lectures at CERN by Werner Riegler

Bremsstrahlung

A charged particle of mass M and charge $q=Z_1e$ is deflected by a nucleus of charge Ze which is partially 'shielded' by the electrons. During this deflection the charge is 'accelerated' and it therefore radiates → Bremsstrahlung.

From Bethe's theory the elastic scattering off the Nucleus is given by

$$\epsilon_0(q) = Z_2 - \sum_{j=1}^{Z_2} \int e^{i(\vec{q}\vec{r}_j)} \psi_0^2(\vec{r}_j) d^3r_1 ... d^3r_{Z_2} = Z_2 - F \qquad \frac{d\sigma}{d\Omega} = \left(\frac{1}{4\pi\varepsilon_0} \frac{Z_1(Z_2 - F)e_0^2}{2pv} \right)^2 \frac{1}{\sin^4 \theta/2}$$

where F(q) describes the partial shielding of the nucleus by the electrons. Effective values for F are used in the following expressions.

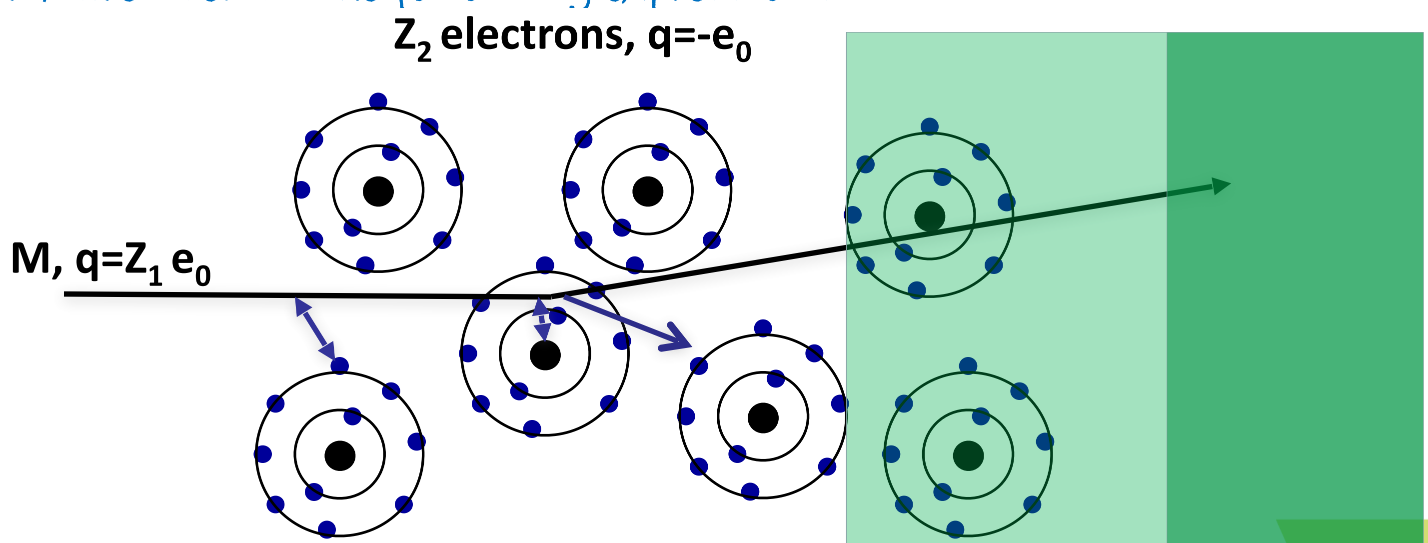

FROM MGA TO NUST MISIS 100 YEARS 1918-2018 OPENING A NEW CENTURY
MISIS National University of Science and Technology
SHiP Search for Hidden Particles
LHCb

Bremsstrahlung: Classical approach

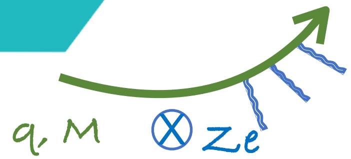

$$q = Z_1 \cdot e$$

$$\frac{d\sigma}{d\Omega} = \left(\frac{2Z_1 Z_2 e^2}{4\pi\epsilon_0\ p \cdot v}\right)^2 \frac{1}{\left(2\sin\frac{\theta}{2}\right)^4}$$

$$p = Mv\gamma$$

"Rutherford Scattering"

Written in Terms of Momentum Transfer: $Q^2 = 2p^2(1-\cos\theta)$

$$\frac{d\sigma}{dQ} = 8\pi\left(\frac{Z_1 Z_2 e^2}{4\pi\epsilon_0 \beta c}\right)^2 \cdot \frac{1}{Q^2}$$

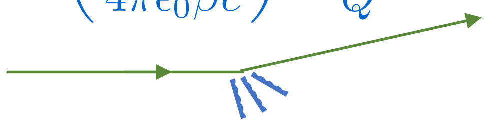

$$Q = |\vec{p} - \vec{p}'|$$

$$\lim_{\omega\to 0}\frac{dI}{d\omega} \sim \frac{2}{3\pi}\frac{Z_1^2 e^2}{M^2 c^3}\frac{Q^2}{4\pi\epsilon_0}$$

Radiated energy between ω and ω'

$$\frac{dE}{dx} = \frac{N_A\rho}{A}\cdot\int_0^{\omega_{max}} d\omega \int_{Q_{min}}^{Q_{max}} dQ \frac{dI}{d\omega}\cdot\frac{d\sigma}{dQ} \qquad \omega_{max} = \frac{E}{\hbar}$$

$$\frac{dE}{dx} = \frac{N_A\rho}{A}\cdot\frac{16}{3}\alpha\cdot Z^2\cdot\left(\frac{Z_1^2 e^2}{4\pi\epsilon_0 M c^2}\right)^2 \cdot E\cdot\ln\frac{Q_{max}}{Q_{min}}$$

$$\alpha = \frac{e^2}{4\pi\varepsilon_0\hbar c} \sim \frac{1}{137}$$

A charged particle of mass M and charge $q = Z_1 e$ is deflected by a nucleus of charge Ze.

Because of the acceleration the particle radiates EM waves → energy loss.

Coulomb-Scattering (Rutherford Scattering) describes the deflection of the particle.

Maxwell's Equations describe the radiated energy for a given momentum transfer.

→ dE/dx

Bremsstrahlung: Quantum Mechanics

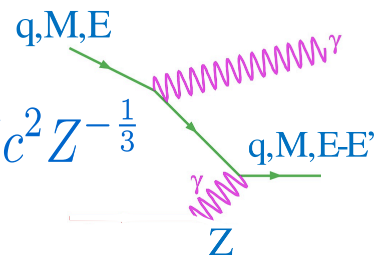

$$q = Z_1 e_1,\ \ E + Mc^2 >> 137 Mc^2 Z^{-\frac{1}{3}}$$

→ Highly Relativistic:

$$\frac{d\sigma(E,E')}{dE'} = 4\alpha Z^2 Z_1^4 \left(\frac{1}{4\pi\epsilon_0}\frac{e^2}{Mc^2}\right)^2 \frac{1}{E'} F(E,E')$$

$$F(E,E') = \left[1 + \left(1 - \frac{E'}{E+Mc^2}\right)^2 - \frac{2}{3}\left(1 - \frac{E'}{E+Mc^2}\right)\right] \ln 183 Z^{-\frac{1}{3}} + \frac{1}{9}\left(1 - \frac{E'}{E+Mc^2}\right)$$

$$\frac{dE}{dx} = -\frac{N_A \rho}{A}\int_0^E E' \frac{d\sigma}{dE'} dE' \sim 4\alpha Z^2 Z_1^4 \left(\frac{1}{4\pi\epsilon_0}\frac{e^2}{Mc^2}\right)^2 E \left[\ln 183 Z^{-\frac{1}{3}} + \frac{1}{18}\right]$$

$$\frac{dE}{dx} = -\frac{N_A \rho}{A} 4\alpha Z^2 Z_1^4 \left(\frac{1}{4\pi\epsilon_0}\frac{e^2}{Mc^2}\right)^2 E \ln\left(183 Z^{-\frac{1}{3}}\right)$$

$$E(x) = E_0 \exp^{-\frac{x}{X_0}}$$

$$X_0 = \frac{A}{4\alpha N_A \rho Z^2 \left(\frac{1}{4\pi\epsilon_0}\frac{e^2}{Mc^2}\right)^2 \ln\left(183 Z^{-\frac{1}{3}}\right)}$$

X_0 radiation length

Proportional to Z^2/A of the Material.

Proportional to Z_1^4 of the incoming particle.

Proportional to ρ of the material.

Proportional $1/M^2$ of the incoming particle.

Proportional to the Energy of the incoming particle →

$E(x)=e(-x/X_0)$ – 'Radiation Length'

$X_0 \propto M^2 A / (\rho Z_1^4 Z^2)$

X_0: Distance where the Energy E_0 of the incoming particle decreases $E_0 e^{-1} = 0.37 E_0$

Critical Energy

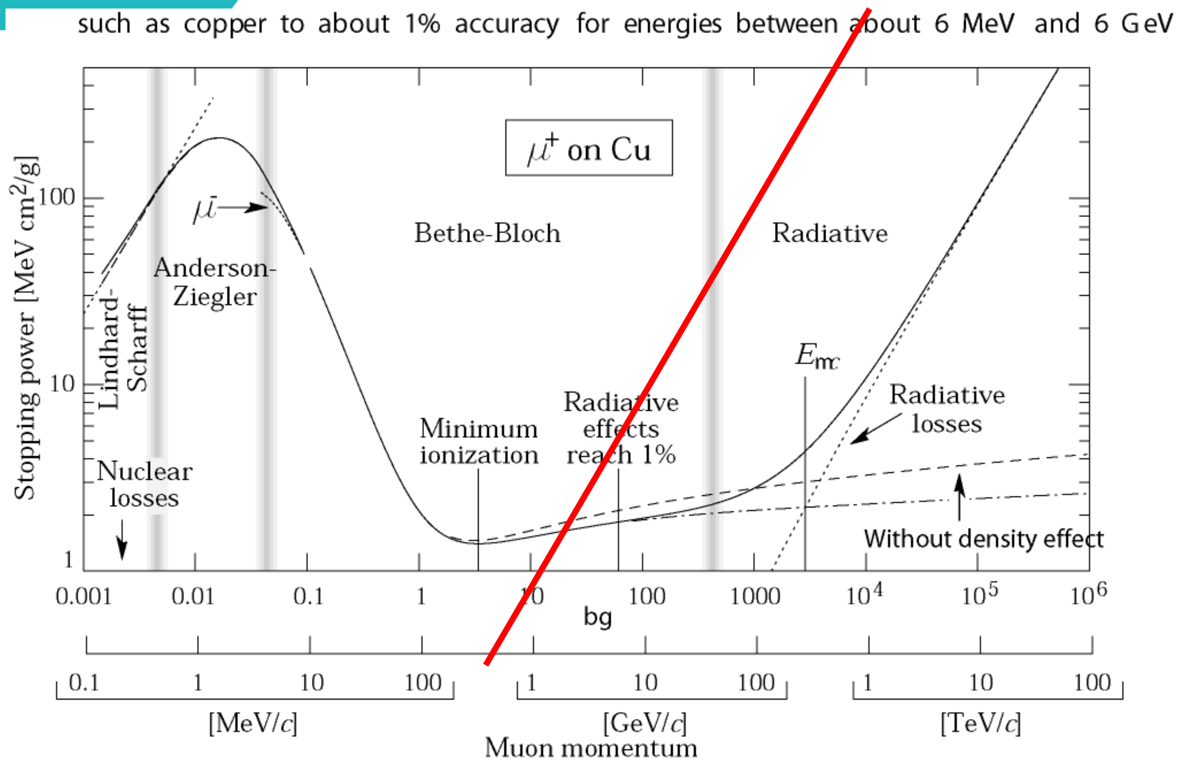

Electron Momentum 5 50 500 MeV/c

For the muon, the second lightest particle after the electron, the critical energy is at 400GeV.

The EM Bremsstrahlung is much less important for muons: at the LHC and in cosmic-rays experiments can be relevant

Critical Energy: If dE/dx (Ionization) = dE/dx (Bremsstrahlung)

Muon in Copper: $p \approx 400$GeV

Electron in Copper: $p \approx 20$MeV

Pair Production: Quantum Mechanics

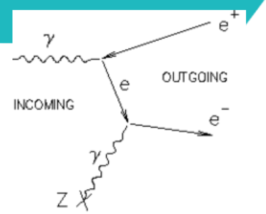

$$\gamma + \text{Nucl.} \to e^+ + e^- + \text{Nucl.}$$

The diagram is very similar to Bremsstrahlung

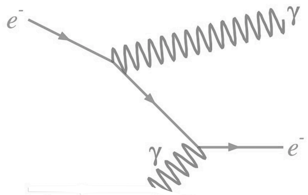

$$e^- + \text{Nucl.} \to \gamma + e^- + \text{Nucl.}$$

Crossing Symmetry:
same cross-section

$$\frac{d\sigma(E,E')}{dE'} = 4\alpha Z^2 r_e^2 \frac{1}{E} \cdot G(E,E') \qquad E >> 137 m_e c^2 Z^{-\frac{1}{3}}$$

$$G(E,E') = \left[\left(\frac{E'+m_e c^2}{E}\right)^2 r \left(1 - \frac{E'+m_e c^2}{E}\right)^2 + \frac{2}{3}\frac{E'+m_e c^2}{E}\left(1 \frac{E'+m_e c^2}{E}\right) \ln Z^{-\frac{1}{3}} - \frac{1}{9}\left(\frac{E'+m_e c^2}{E}\right)\left(1 - \frac{E'+m_e c^2}{E}\right)\right]$$

$$\sigma = \int_0^{E-2m_e c^2} \frac{d\sigma'}{dE'} dE' = 4\alpha Z^2 r_e^2 \cdot \frac{7}{9} \ln 183 Z^{-\frac{1}{3}}$$

$$P(x) = \frac{1}{\lambda} e^{-\frac{x}{\lambda}} \qquad \lambda = \frac{A}{\rho N_A \sigma} = \frac{9}{7} X_0$$

Probability that Photon converts to e^+e^- after a distance x

For $E\gamma >> m_e c^2 = 0.5$ MeV : $\lambda = 9/7 X_0$

Average distance a high energy photon has to travel before it converts into an e^+e^- pair is equal to 9/7 of the distance that a high energy electron has to travel before reducing its energy from E_0 to $E_0 * e^{-1}$ by photon radiation.

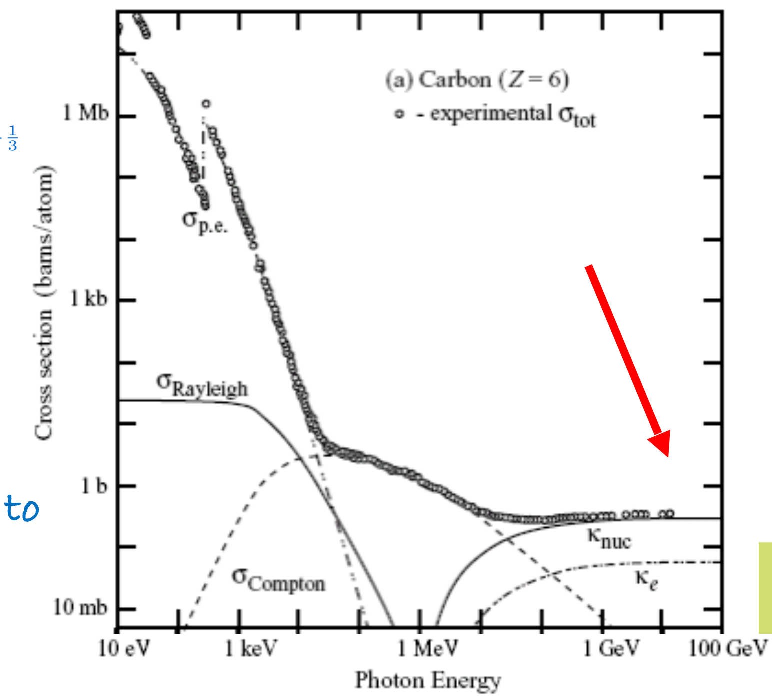

Bremsstrahlung + Pair Production → EM Shower

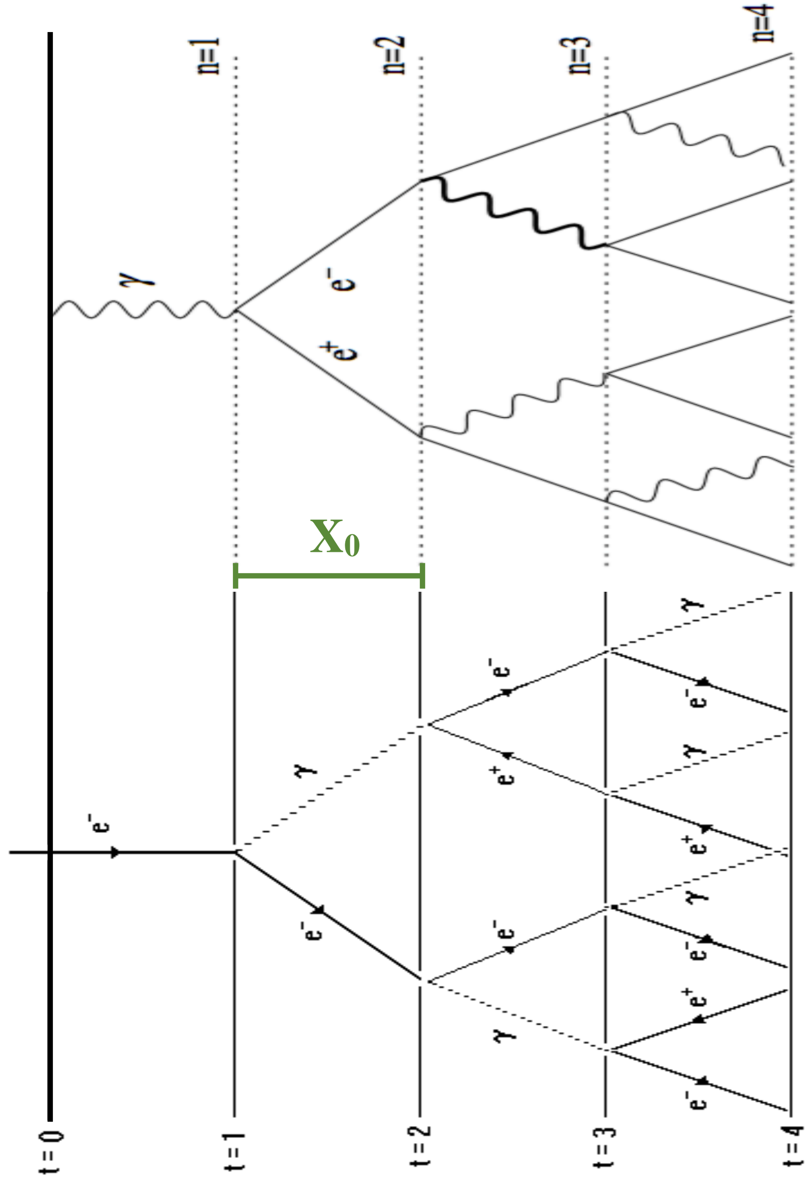

Electromagnetic Shower → EM Calorimeter

FROM MGA TO NUST MISIS
100 YEARS
1918-2018
OPENING A NEW CENTURY
MISIS
National University of Science and Technology

Electro-Magnetic Shower of High Energy Electrons and Photons

$$N(n) = 2^n$$ Number of particles ($e^\pm$,γ) after nX_0

$$E(n) = \frac{E_0}{2^n}$$ Average Energy of particles after nX_0

Shower stops if $E(n) = E_c$

$$n_{max} = \frac{1}{\ln 2} \ln \frac{E_0}{E_c}$$ Shower length rises with $\ln E_0$

$$N_{tr}(n) = 2^n$$ Number of $e^\pm$ track segments of length X_0 after nX_0

$$L = \sum_{n=0}^{n_{max}} 2^n X_0 = \left(2\frac{E_0}{E_c} - 1\right) X_0 \sim 2\frac{E_0}{E_c} X_0 = c_1 \cdot E_0$$

Total (charged) track length is proportional to the Energy of the particle

→ Calorimeter Principle

Calorimetry: Energy Measurement by total Absorption of Particles

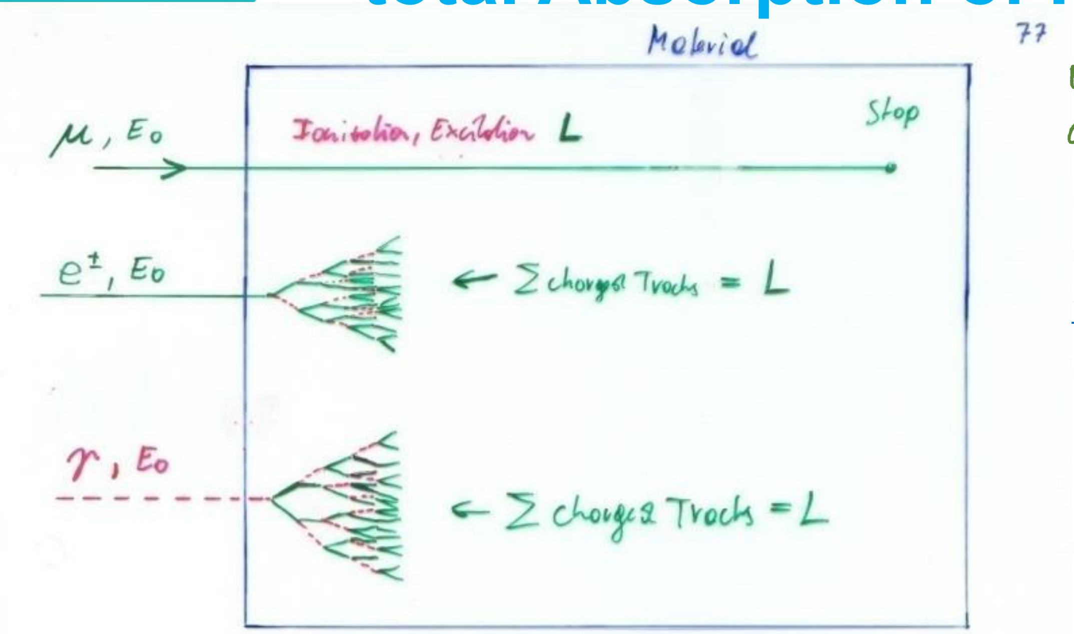

If N is the total number of e^-, I^+ pairs or photons, $N = c_1 E_0$:

$$\Delta N = \sqrt{N} \quad \text{(Poisson statistics)}$$

$$\frac{\Delta E}{E} = \frac{\Delta N}{N} = \frac{1}{\sqrt{N}} = \frac{a}{\sqrt{E}}$$

Radiation

The $e^{\pm}$ in the Calorimeter ionize and excite the material

Ionization: e^-, I^+ pairs in the material

Excitation: Photons in the material

Measuring the total number of e^-, I^+ pairs or the total number of photons gives the particle Energy

Only Electrons and High Energy Photons show EM cascades at current GeV-TeV level Energies.

Strongly interacting particles like Pions, Kaons, produce hadronic showers in a similar fashion to the EM cascade → Hadronic calorimetry

Calorimetry: Energy Measurement by total Absorption of Particles

The measurement is destructive. The particle cannot be studied further

Energy measurement by:

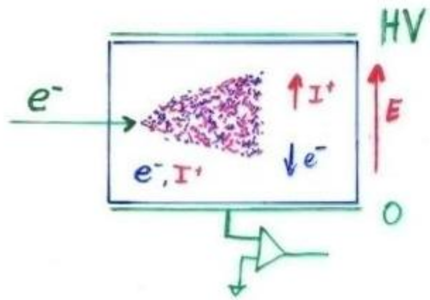

Collecting the produced charge

Liquid Noble Gas

(Noble Liquids)

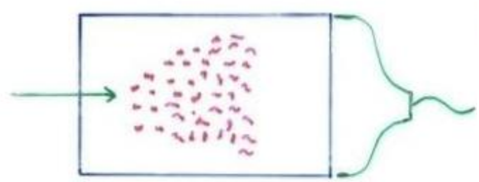

Measuring the photons produced by the collisions of the e± with the atom electrons of the material

Scintillating Crystals,

Plastic Scintillators

Total amount of pairs or photons is proportional to the total track length and is proportional to the particle energy

FROM MGA TO NUST MISIS 100 YEARS 1918-2018 OPENING A NEW CENTURY
MISIS National University of Science and Technology
SHiP Search for Hidden Particles
LHCb

Calorimetry

Calorimeters are blocks of instrumented material in which particles to be measured are fully absorbed and their energy transformed into a measurable quantity.

The interaction of the incident particle with the detector (through electro-magnetic or strong processes) produces a shower of secondary particles with progressively degraded energy.

The energy deposited by the charged particles of the shower in the active part of the calorimeter, which can be detected in the form of charge or light, serves as a measurement of the energy of the incident particle.

C.W. Fabjan and F. Gianotti, Rev. Mod. Phys., Vol. 75, N0. 4, October 2003

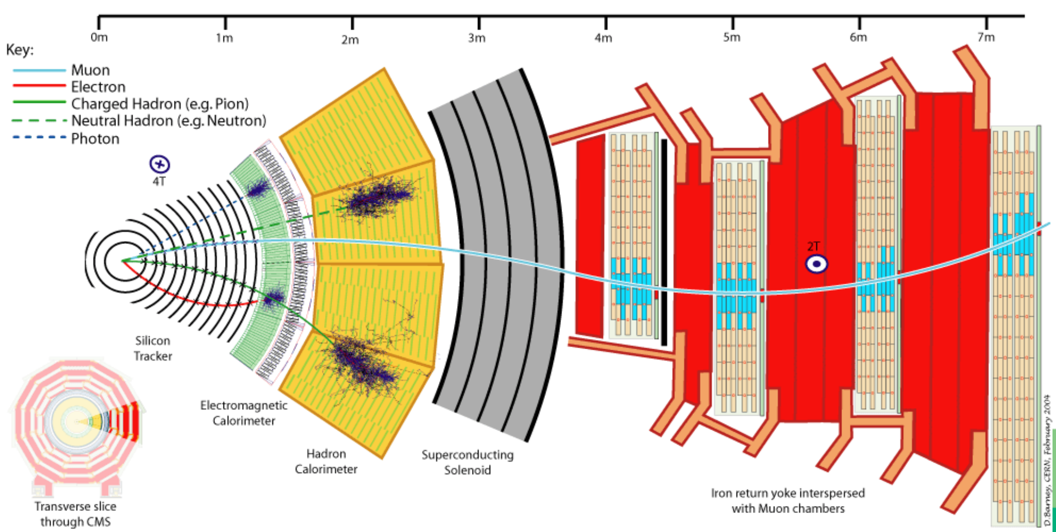

Calorimetry

Calorimeters can be classified into:

- Electromagnetic Calorimeters,
  to measure electrons and photons through their EM interactions.
- Hadron Calorimeters,
  Used to measure hadrons through their strong and EM interactions.

The construction can be classified into:

- Homogeneous Calorimeters,
  that are built of only one type of material that performs both tasks, energy degradation and signal generation.
- Sampling Calorimeters,
  that consist of alternating layers of an absorber, a dense material used to degrade the energy of the incident particle, and an active medium that provides the detectable signal.

C.W. Fabjan and F. Gianotti, Rev. Mod. Phys., Vol. 75, N0. 4, October 2003

Calorimetry

Calorimeters are attractive in our field for various reasons:

In contrast with magnet spectrometers, in which the momentum resolution deteriorates linearly with the particle momentum, on most cases the calorimeter energy resolution improves as 1/Sqrt(E), where E is the energy of the incident particle. Therefore calorimeters are very well suited for high-energy physics experiments.

In contrast to magnet spectrometers, calorimeters are sensitive to all types of particles, charged and neutral. They can even provide indirect detection of neutrinos and their energy through a measurement of the event missing energy.

Calorimeters are commonly used for trigger purposes since they can provide fast signals that are easy to process and interpret.

They are space and therefore cost effective. Because the shower length increases only logarithmically with energy, the detector thickness needs to increase only logarithmically with the energy of the particles. On the contrary, for a fixed momentum resolution, the bending power BL^2 of a magnetic spectrometer must increase linearly with the particle momentum.

C.W. Fabjan and F. Gianotti, Rev. Mod. Phys., Vol. 75, N0. 4, October 2003

Interaction of Particles with Matter

Any device to detect a particle must interact with it in some way → almost …

Neutrinos can be measured by missing transverse energy.

E.g. p p collider $E_T=0$,

If the ΣE_T of all collision products is $\neq 0$ → neutrino escaped

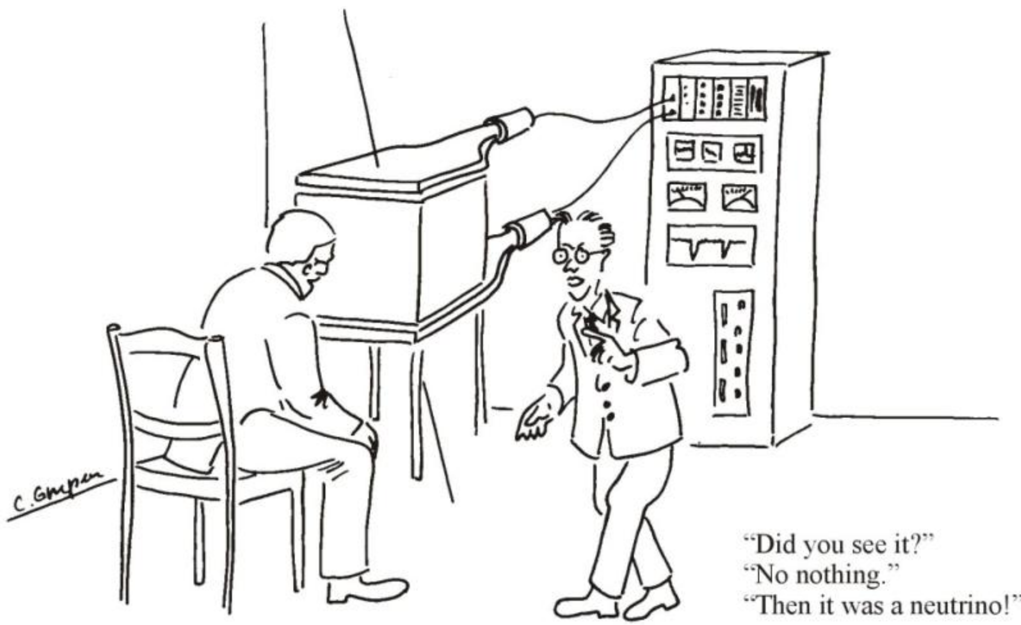

Claus Grupen, Particle Detectors, Cambridge University Press, 1996

EM Calorimetry

Approximate longitudinal shower development

$$N(n) = 2^n$$

Number of particles ($e^{\pm}$,γ) after nX_0

$$E(n) = \frac{E_0}{2^n}$$

Average Energy of particles after nX_0

Shower stops if $E(n) = E_c$

$$n_{max} = \frac{1}{\ln 2} \ln \frac{E_0}{E_c}$$

Shower length rises with $\ln E_0$

Radiation Length X_0 and Moliere Radius are two key parameters for the choice of calorimeter materials

Approximate transverse shower development

The traverse shower direction is mainly related to the Multiple Coulomb Scattering of the low Energy Electrons

$$\theta_0 \sim \frac{21(mrad)}{\beta p\,(MeV)} Z_1 \sqrt{\frac{X}{X_0}}$$

Electrons: $E_c,\ E \sim p \cdot c$

$$\theta_0 \sim \frac{21(mrad)}{\beta E_c\,(MeV)} Z_1 \sqrt{\frac{X}{X_0}} \qquad Z_1 = 1,\ \beta \sim 1$$

$$E_c \sim \frac{610}{Z + 1.24} MeV \sim \frac{610}{Z} MeV$$

$$\theta = 0.0344 \cdot Z \cdot \sqrt{\frac{X}{X_0}}$$

Moliere Radius ρ_m = Lateral Shower Radius after $1X_0$

$$\rho_m \approx 0.0344 \cdot Z \cdot X_0$$

95% of Energy is in a Cylinder of $2\rho_m$ radius

Simulated EM Shower Profiles in $PbWO_4$

Simulation of longitudinal shower profile   Simulation of transverse shower profile

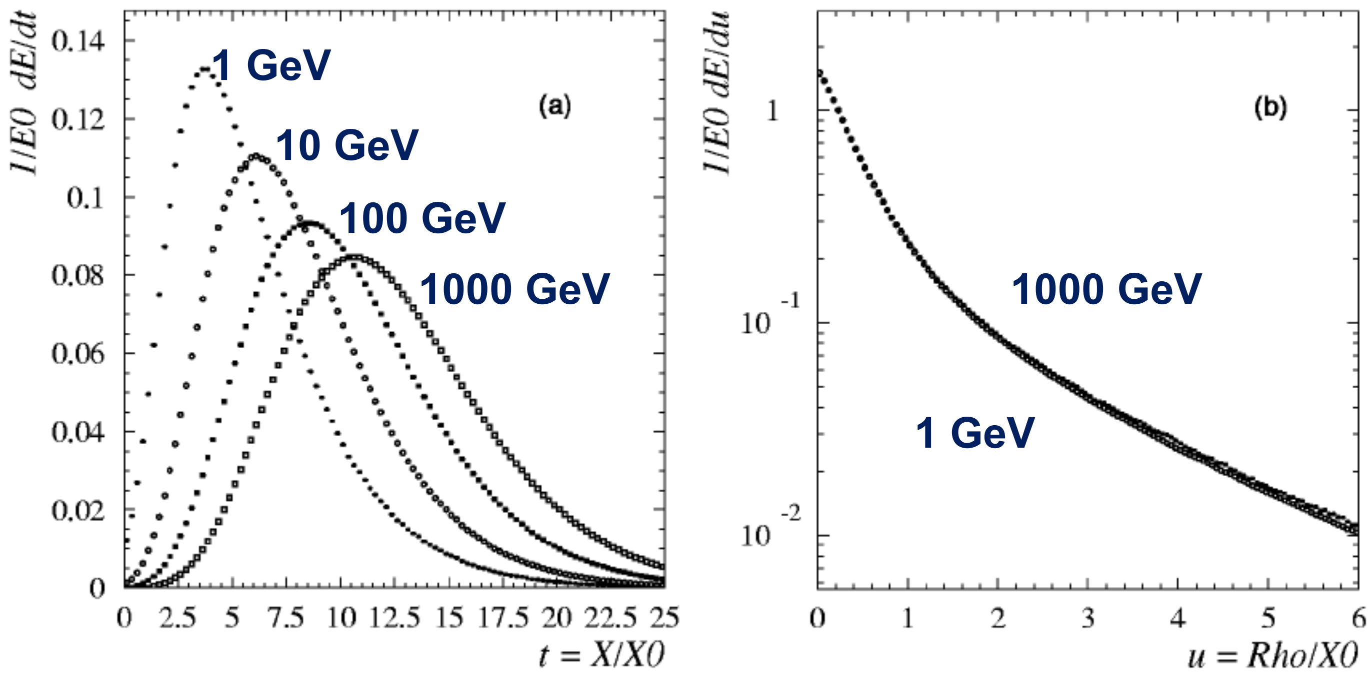

FIG. 2. (a) Simulated shower longitudinal profiles in $PbWO_4$, as a function of the material thickness (expressed in radiation lengths), for incident electrons of energy (from left to right) 1 GeV, 10 GeV, 100 GeV, 1 TeV. (b) Simulated radial shower profiles in $PbWO_4$, as a function of the radial distance from the shower axis (expressed in radiation lengths), for 1 GeV (closed circles) and 1 TeV (open circles) incident electrons. From Maire (2001).

In calorimeters with thickness ~ 25 X_0, the shower leakage beyond the end of the active detector is much less than 1% up to incident electron energies of ~ 300 GeV (LHC energies).

FROM MGA TO NUST MISIS 100 YEARS 1918-2018 OPENING A NEW CENTURY | MISIS National University of Science and Technology | SHiP Search for Hidden Particles | LHCb

Crystals for Homogeneous EM Calorimetry

In crystals the light emission is related to the crystal structure of the material. Incident charged particles create electron-hole pairs and photons are emitted when electrons return to the valence band.

The incident electron or photon is completely absorbed and the produced amount of light, which is reflected through the transparent crystal, is measured by photomultipliers (PM) or solid state photon detectors (SiPM)

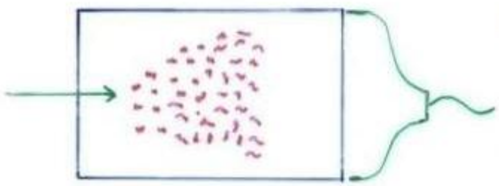

Measuring the Photons produced by the collision of the $e^{\pm}$ with atom electrons of the material

Crystals for Homogeneous EM Calorimetry

	NaI(Tl)	CsI(Tl)	CsI	BGO	$PbWO_4$
Density (g/cm^3)	3.67	4.53	4.53	7.13	8.28
X_0 (cm)	2.59	1.85	1.85	1.12	0.89
R_M (cm)	4.5	3.8	3.8	2.4	2.2
Decay time (ns)	250	1000	10	300	5
slow component			36		15
Emission peak (nm)	410	565	305	410	440
slow component			480		
Light yield γ/MeV	4×10^4	5×10^4	4×10^4	8×10^3	1.5×10^2
Photoelectron yield (relative to NaI)	1	0.4	0.1	0.15	0.01
Rad. hardness (Gy)	1	10	10^3	1	10^5

Babar@PEPII, 10ms interaction rate, good light yield, good S/N

KTeV@Tevatron, High rate, Good resolution

L3@LEP, 25us bunch crossing, Low radiation dose

CMS@LHC, 25ns bunch crossing, high radiation dose

MISIS National University of Science and Technology

Crystals for Homogeneous EM Calorimetry

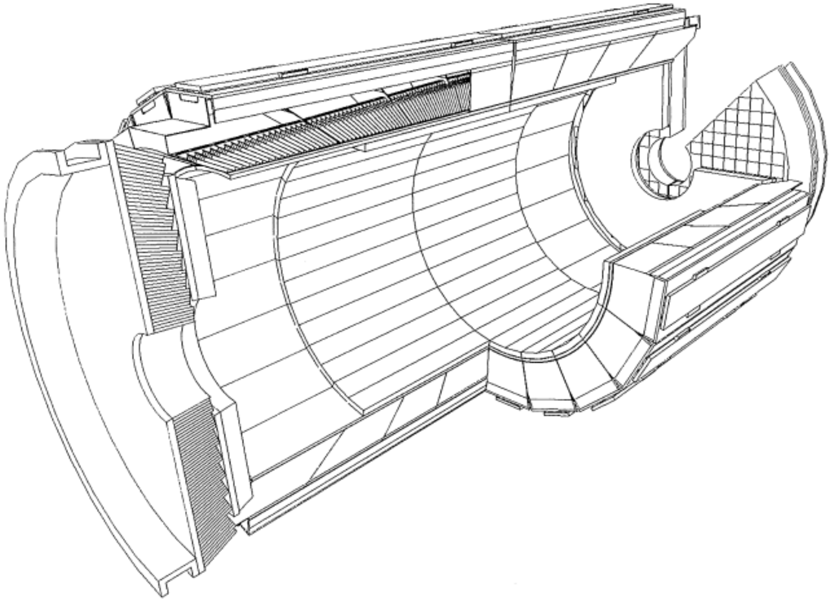

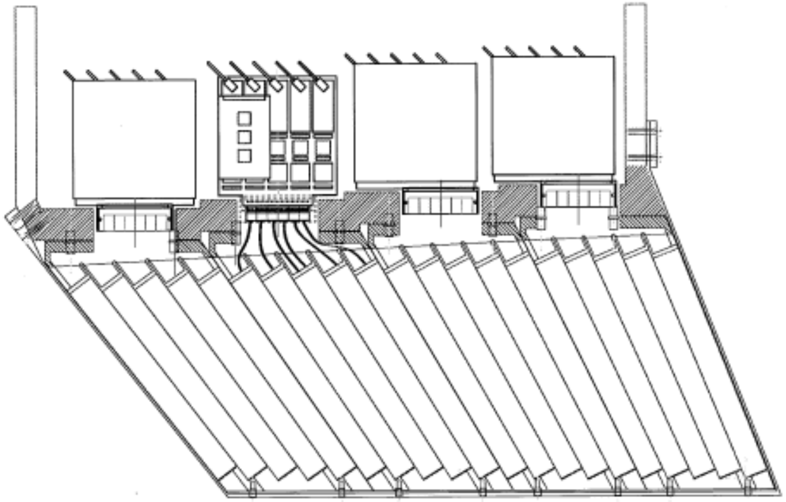

Fig. 2. Longitudinal drawing of module 2, showing the structure and the front-end electronics layout.

FROM MGA TO NUST MISIS 100 YEARS 1918-2018 OPENING A NEW CENTURY
MISIS National University of Science and Technology
SHiP Search for Hidden Particles
LHCb

Noble Liquids for Homogeneous EM Calorimetry

	Ar	Kr	Xe
Z	18	36	58
A	40	84	131
X_0 (cm)	14	4.7	2.8
R_M (cm)	7.2	4.7	4.2
Density (g/cm^3)	1.4	2.5	3.0
Ionization energy (eV/pair)	23.3	20.5	15.6
Critical energy ϵ (MeV)	41.7	21.5	14.5
Drift velocity at saturation (mm/μs)	10	5	3

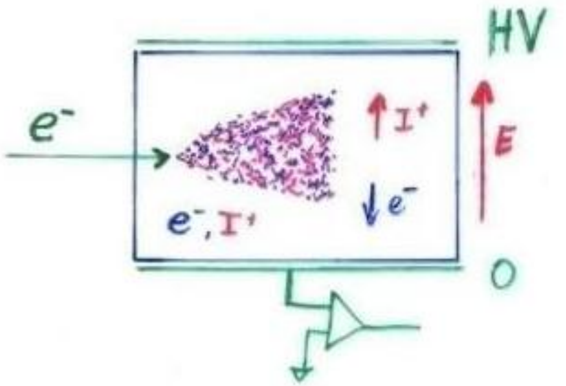

When a charge particle traverses these materials, about half the lost energy is converted into ionization and half into scintillation.

The best energy resolution would obviously be obtained by collecting both the charge and light signal. This is however rarely done because of the technical difficulties to extract light and charge in the same instrument.

Krypton is preferred in homogeneous detectors due to small radiation length and therefore compact detectors. Liquid Argon is frequently used due to low cost and high purity in sampling calorimeters.

FROM MGA TO NUST MISIS 100 YEARS 1918-2018 OPENING A NEW CENTURY | MISIS National University of Science and Technology | SHiP Search for Hidden Particles | LHCb

Noble Liquids for Homogeneous EM Calorimetry

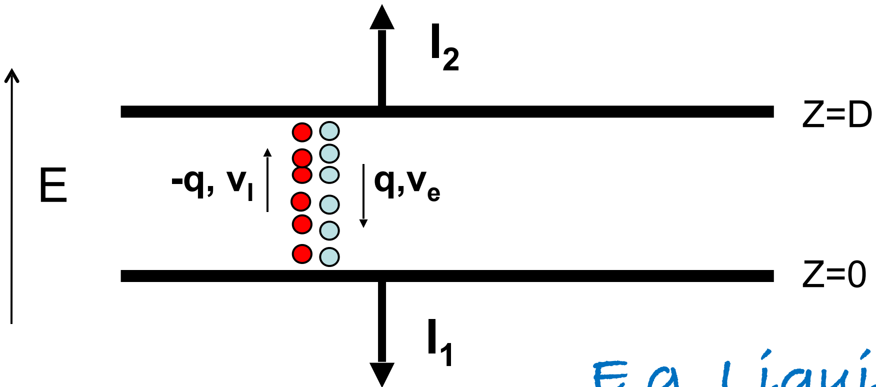

E.g. Liquid Argon, 5mm/μs at 1kV/cm, 5mm gap → 1μs for all electrons to reach the electrode.

The ion velocity is 10^3 to 10^5 times smaller → doesn't contribute to the signal for electronics of μs integration time.

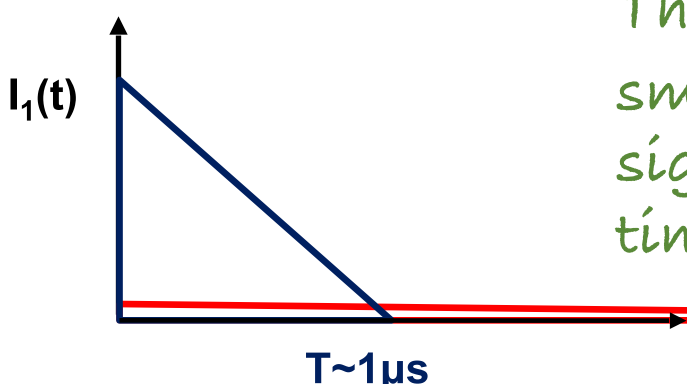

Homogeneous EM Calorimeters, Examples

NA48 Liquid Krypton
2cmx2cm cells
X_0 = 4.7cm
125cm length (27X_0)
ρ = 5.5cm

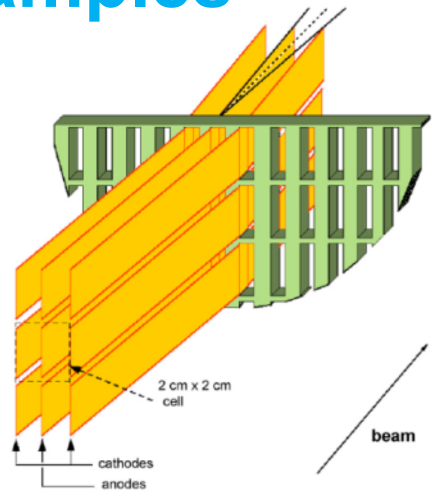

KTeV CsI
5cmx5cm and
X_0 = 1.85cm
2.5cmx2.5cm crystals
50cm length (27X_0)
ρ = 3.5cm

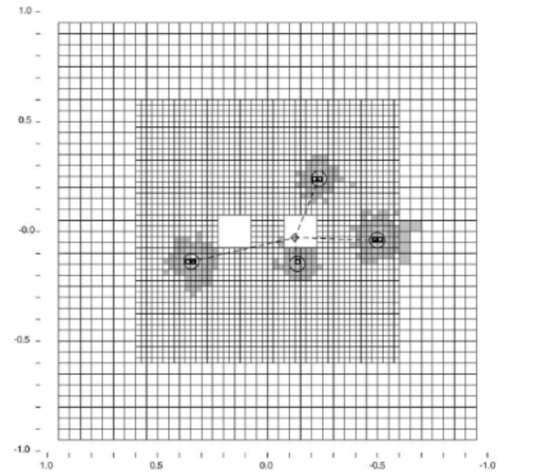

Fig. 1. Schematic of the KTeV CsI Calorimeter showing the cluster energy profiles due to four photons.

NA48 Experiment at CERN and KTeV Experiment at Fermilab, both built for measurement of direct CP violation. Homogenous calorimeters with Liquid Krypton (NA48) and CsI (KTeV). Excellent and very similar resolution.

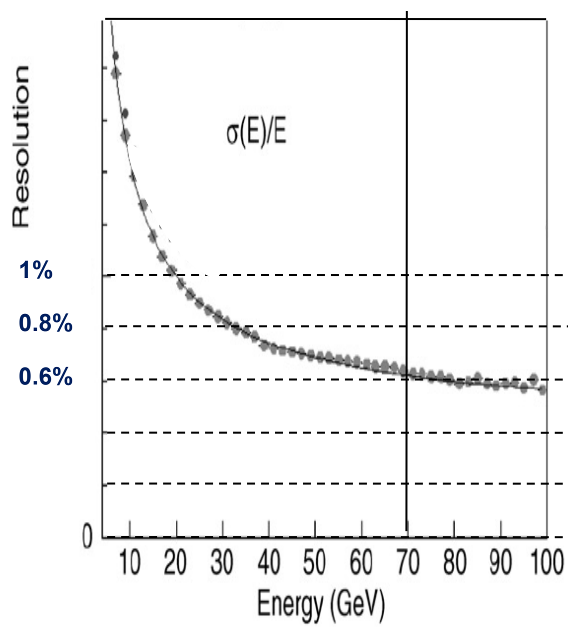

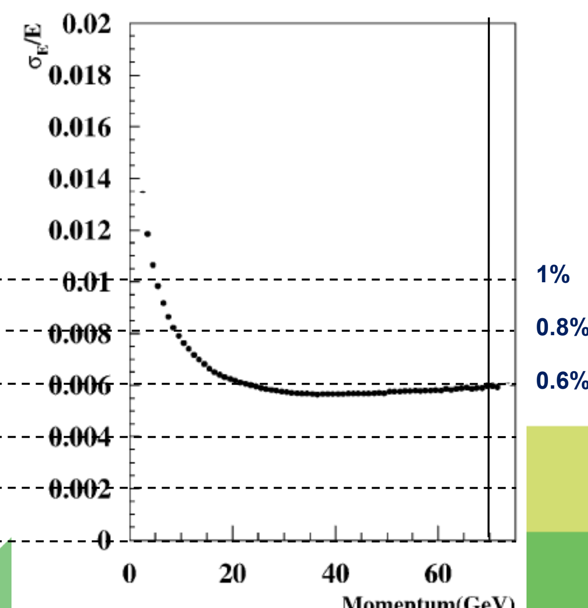

MISIS National University of Science and Technology
FROM MGA TO NUST MISIS 100 YEARS 1918-2018 OPENING A NEW CENTURY
SHiP Search for Hidden Particles

Energy Resolution of Calorimeters

Stochastic term:
Fluctuations related to the physics development of the shower.

Noise term:
From electronics noise of the readout chain. For constant electronics noise → double signal = double S/N

Constant term:
Instrumental effects that cause variations of the calorimeter response with the particle impact point.

$$\frac{\sigma}{E} = \frac{a}{\sqrt{E}} \oplus \frac{b}{E} \oplus c$$

Add in squares

For homogeneous calorimeters the noise term and constant term become dominant.

For sampling calorimeters the stochastic term, then called 'sampling' term becomes dominant.

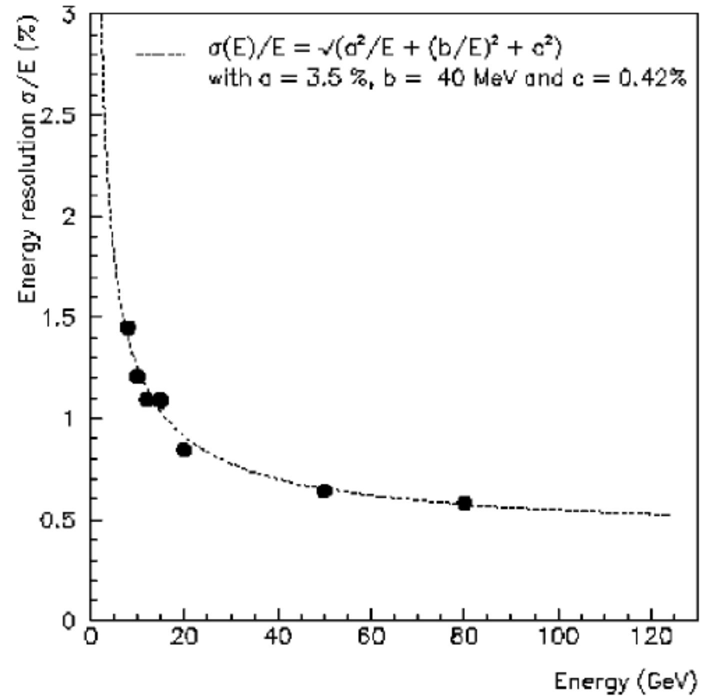

FIG. 3. Fractional electron energy resolution as a function of energy measured with a prototype of the NA48 liquid krypton electromagnetic calorimeter (NA48 Collaboration, 1995). The line is a fit to the experimental points with the form and the parameters indicated in the figure.

Sampling Calorimeters

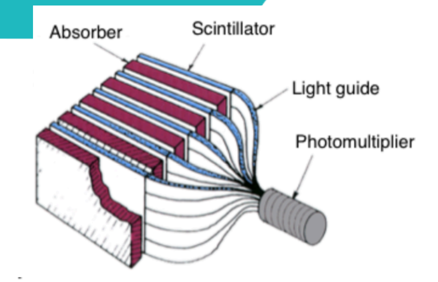

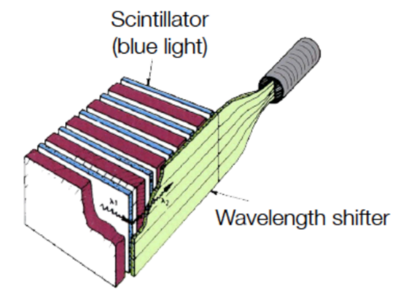

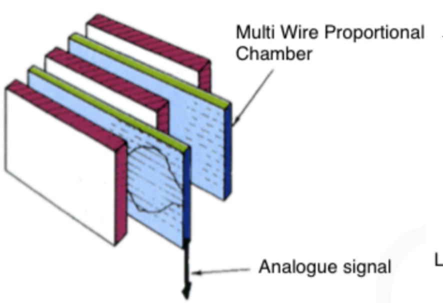

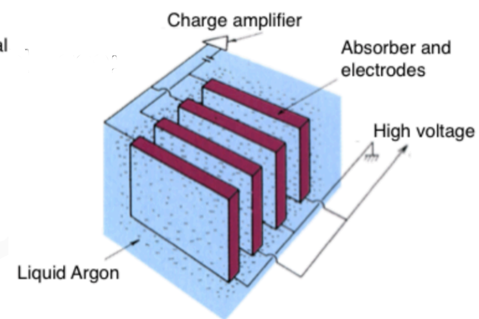

Alternation of "passive" absorber plates and "active" readout sections

Advantage:

- optimum choice of absorber material
- optimum choice of signal readout
- compact and cheap construction

"passive": Pb, Fe…

"active": Scintillator (signal → Photons)

Noble Liquid, e.g. Ar (Signal → e^-, I^-)

Wire Chambers (Signal → e^-, I^+)

Emulsions (Signal —> tracks)

Energy resolution of sampling calorimeters is in general worse than that of homogeneous calorimeters, owing to the sampling fluctuations – the fluctuation of ratio of energy deposited in the active and passive material.

The resolution is in the range 5-20%/Sqrt[E(GeV)] for EM calorimeters. On the other hand they are relatively easy to segment longitudinally and laterally and therefore they usually offer better space resolution and particle identification than homogeneous calorimeters.

Active medium can be scintillators, solid state detectors, emulsion films, gas detectors or liquids.

Sampling Fraction = Energy deposited in Active/Energy deposited in passive material.

Gas and Solid State Sampling Calorimeters

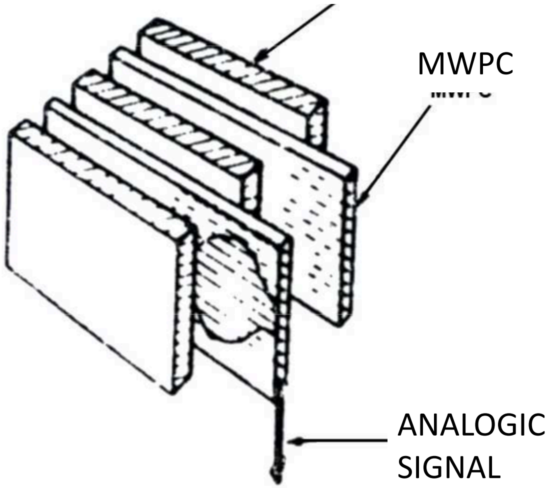

Gas sampling calorimeters have been widely employed at LEP because of their low cost and segmentation flexibility.

They are not well suited to present and future machines because of their modest EM energy resolution ~ 20%/Sqrt[E(GeV)].

Solid state detectors as active readout medium use mostly silicon. The advantage is very high signal to noise ratio (large signals). Often used on a small scale as luminosity monitors.

The disadvantage is the high cost, preventing large calorimeters, and modest radiation resistance.

Scintillator Sampling Calorimeters

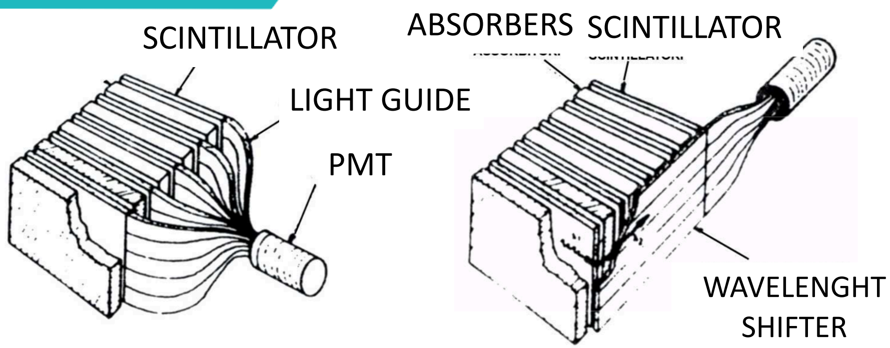

Wavelength shifters absorb photons from the scintillators and emit light at a longer wavelength which does not go back into the scintillator but is internally reflected along the readout plate to the photon detector → compact design.

A large number of sampling calorimeters use organic scintillators arranged in fibers or plates.

The drawbacks are that the optical readout suffers from radiation damage and non-uniformities at various stages are often the source of a large constant term.

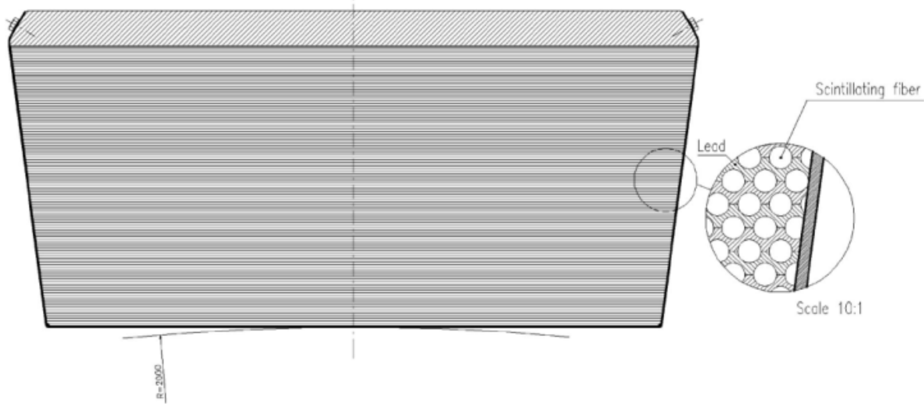

FIG. 13. Schematic layout of the barrel part of the KLOE electromagnetic calorimeter (Antonelli *et al.*, 1995).

KLOE EM calorimeter:

$$\frac{5\%}{\sqrt{E(GeV)}}$$

Liquid Sampling Calorimeters

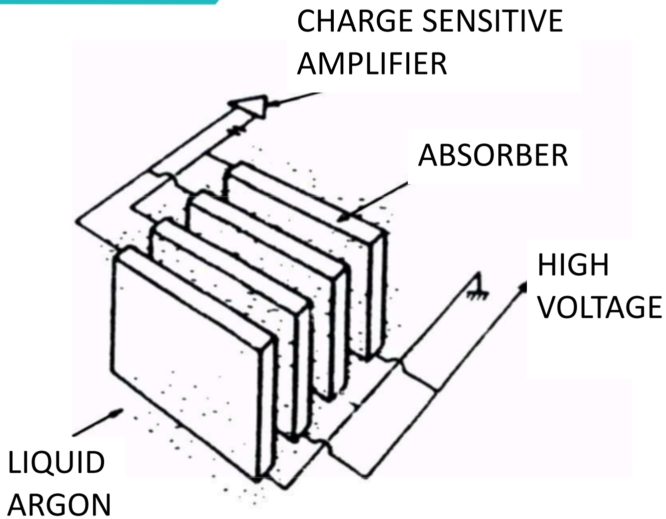

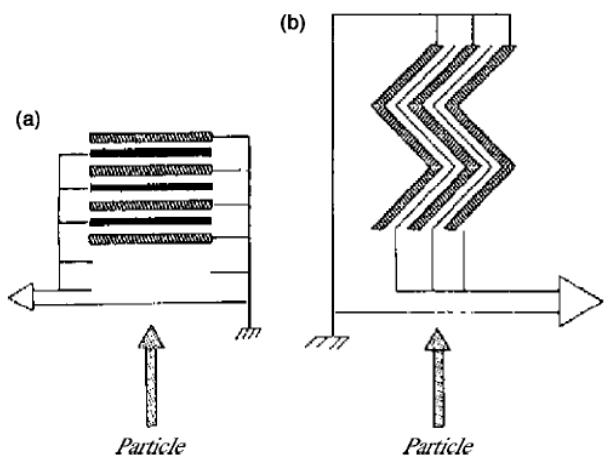

FIG. 15. Schematic view of a traditional sampling calorimeter geometry (a) and of the accordion calorimeter geometry (b).

Liquids at room temperature do not require cryogeny but are characterized by poor radiation resistance and suffer from purity problems

→Noble liquids at cryogenic temperatures.

The advantages are operation in 'ion chamber mode', i.e. deposited charge is large and doesn't need multiplication, which ensures better uniformity compared to gas calorimeters that need amplification.

They are relatively uniform and easy to calibrate because the active medium is homogeneously distributed inside the volume. They provide good energy resolution (e.g. ATLAS 10%/Sqrt[E(GeV)])

And stable operation with time.

They are radiation hard.

With the standard liquid argon sampling calorimeters the alternating absorber and active layers are placed perpendicular to the direction of the incident particle.

→ Long cables are needed to gang together the readout electrodes, causing signal degradation, dead spaces between the calorimeter towers and therefore reduced hermeticity.

Liquid Argon Sampling Calorimeters

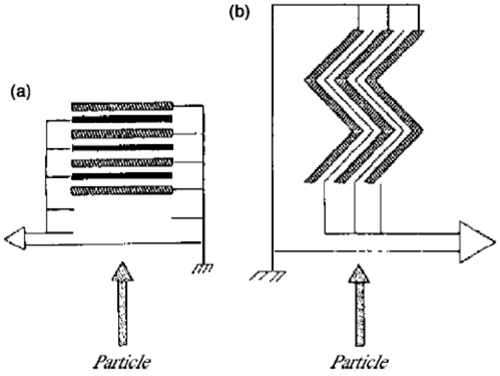

FIG. 15. Schematic view of a traditional sampling calorimeter geometry (a) and of the accordion calorimeter geometry (b).

For the ATLAS LAr Calorimeter this was solved by placing the absorbers in an accordion geometry parallel to the particle direction and the electrodes can be read out from the 'back side'.

ATLAS: Lead layers of 1.1-2.2mm, depending on the rapidity region, separated by 4mm liquid Argon gaps.

Test beam results have shown

10%/Sqrt[E(GeV)]   x 0.25/E(GeV)   x 0.3%

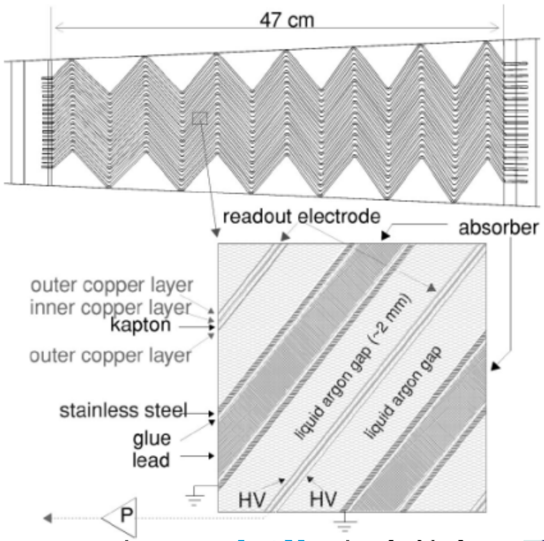

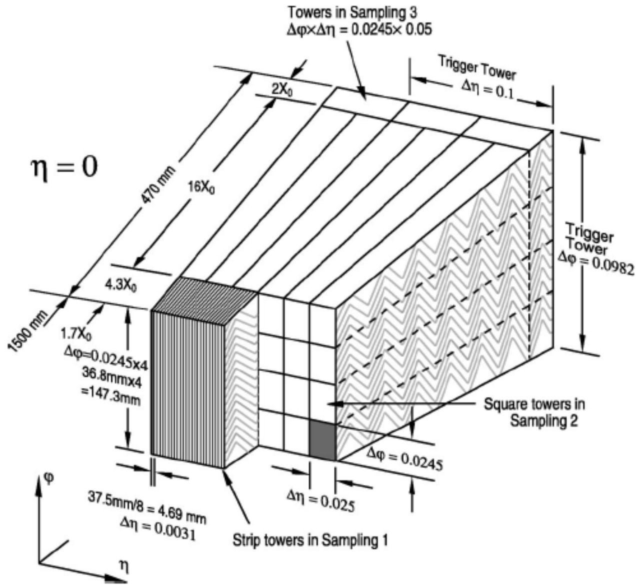

FIG. 17. Schematic view of the segmentation of the ATLAS electromagnetic calorimeter.

Emulsion Cloud Chamber: a peculiar type of sampling calorimeter

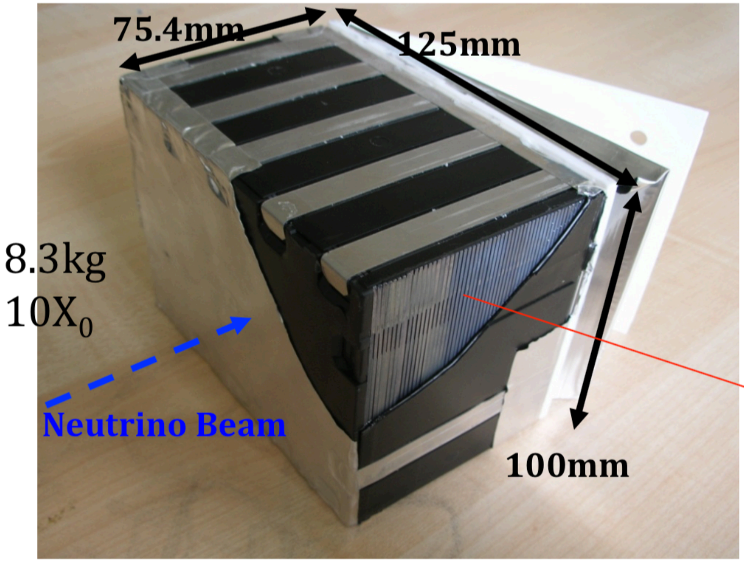

One brick:

- 57 emulsion films
- 56 Pb plates
- a box with a removable pair of films called Changeable Sheets

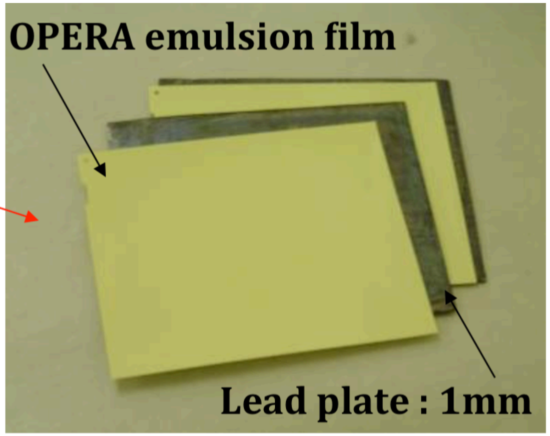

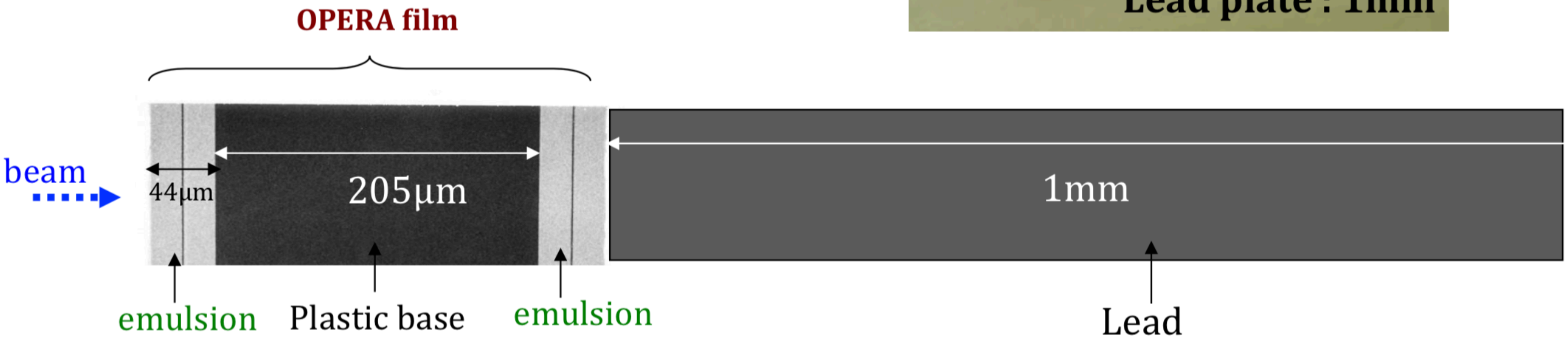

Electromagnetic showers as seen in an Emulsion Cloud Chamber: e/π^0 separation

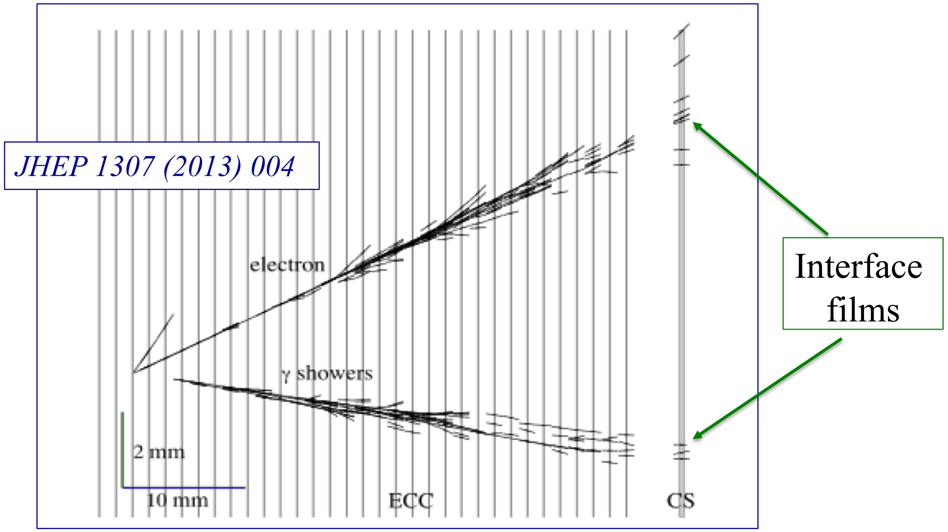

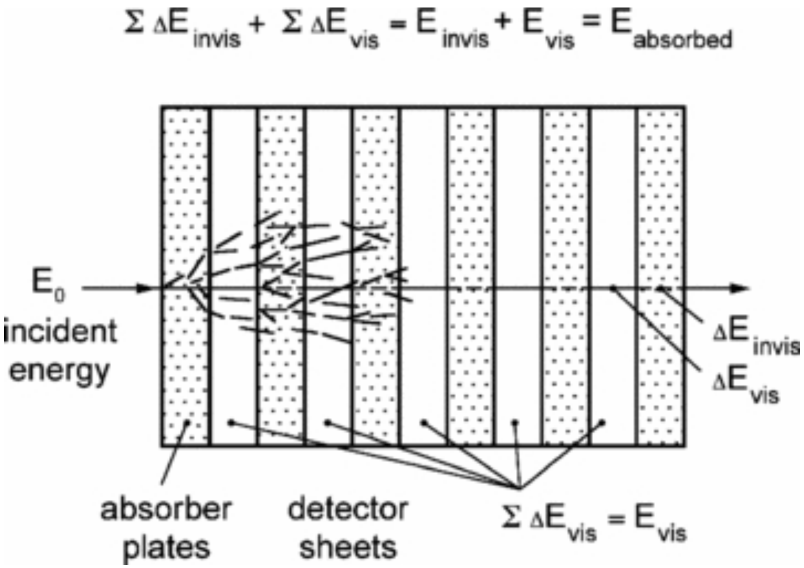

High sampling frequency, 6 active layers every X^0

—> high spatial resolution —> high purity in e/π^0 separation

Electron neutrino interaction with a π^0

Transverse plane

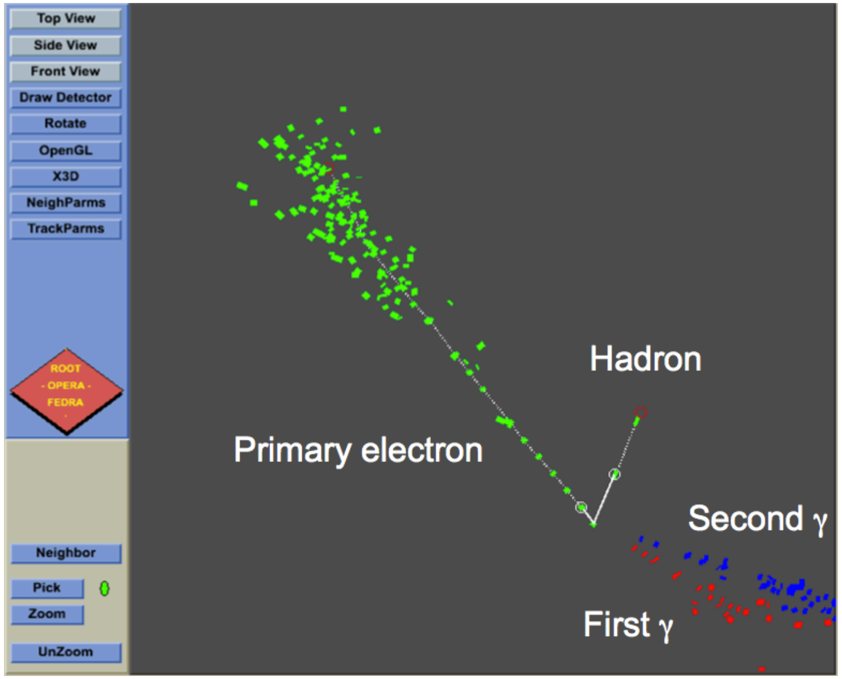

Side view

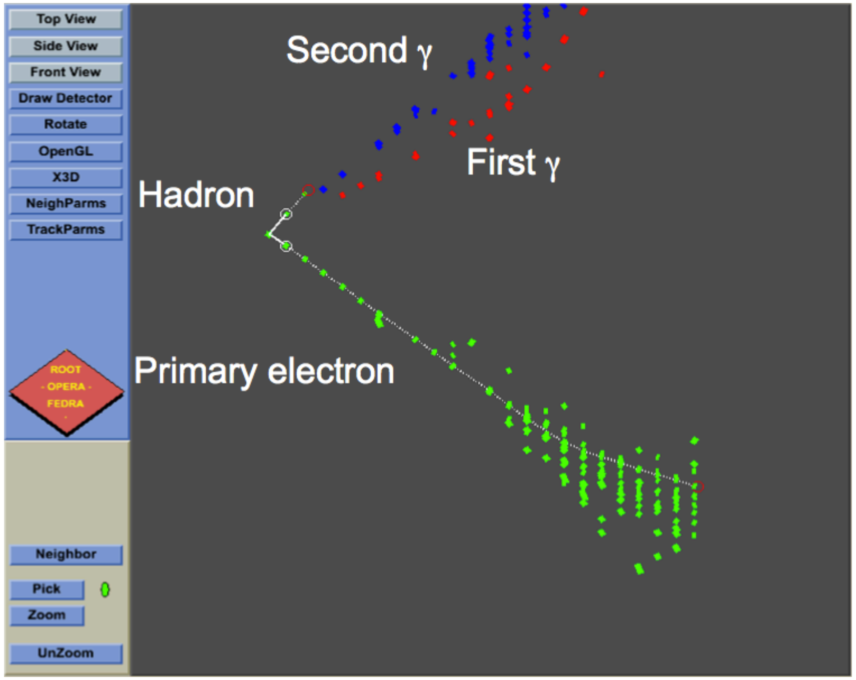

Algorithms for shower and energy reconstruction

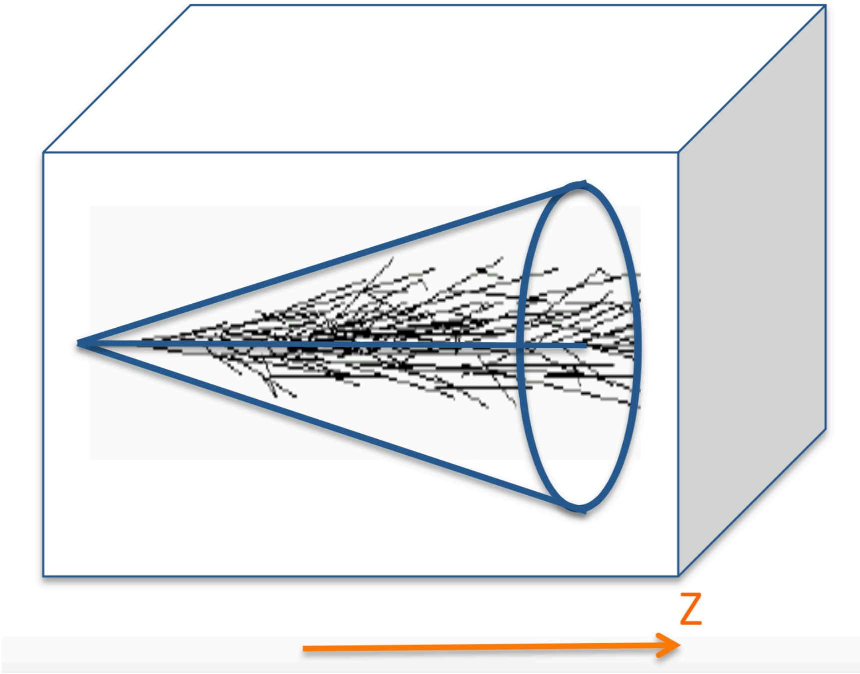

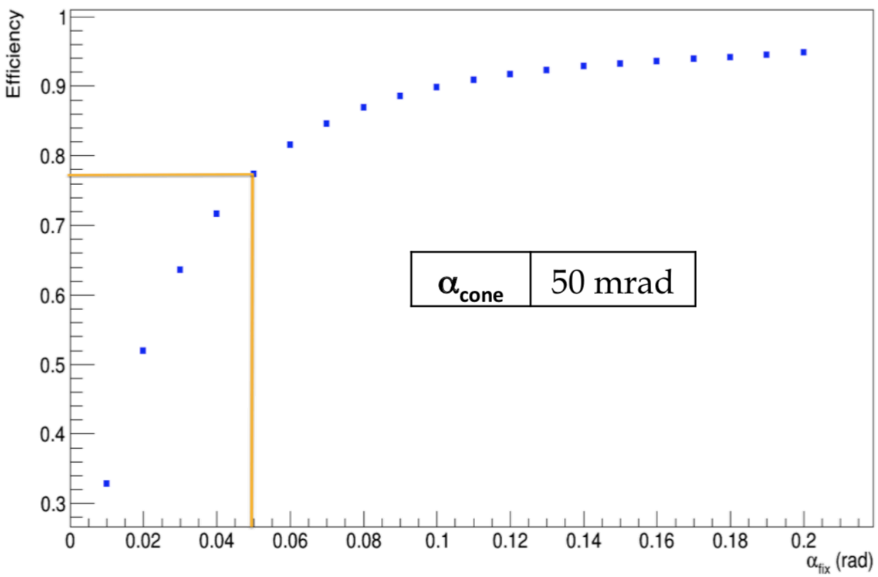

$$\text{Efficency} = \frac{\text{Number of the tracks inside the cone for a given opening angle}}{\text{Total Number of tracks related to the shower}}$$

Variables Used to discard the Instrumental Background

1. Alpha:

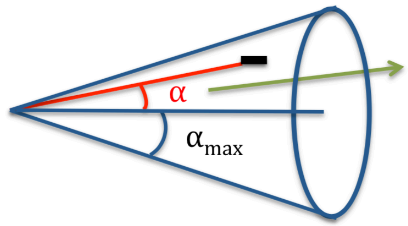

Alpha is calculated for all BTs

α_{max} = 50 mrad

$0 < \alpha < 50$ mrad

2. Impact Parameter divided by the distance from the decay vertex:

$$IPA = \frac{IP}{\Delta z}$$

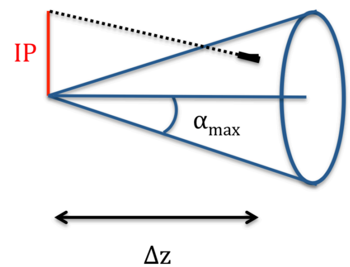

3, 4. ΔSx, ΔSy:

- $\Delta Sx = Sx_e - Sx_i$
- $\Delta Sy = Sy_e - Sy_i$

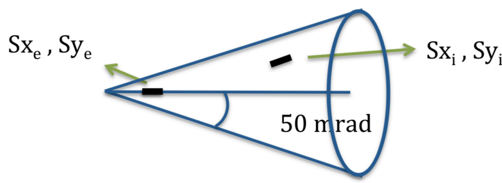

5. χ^2:

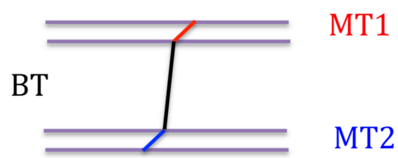

Different performance in different zones

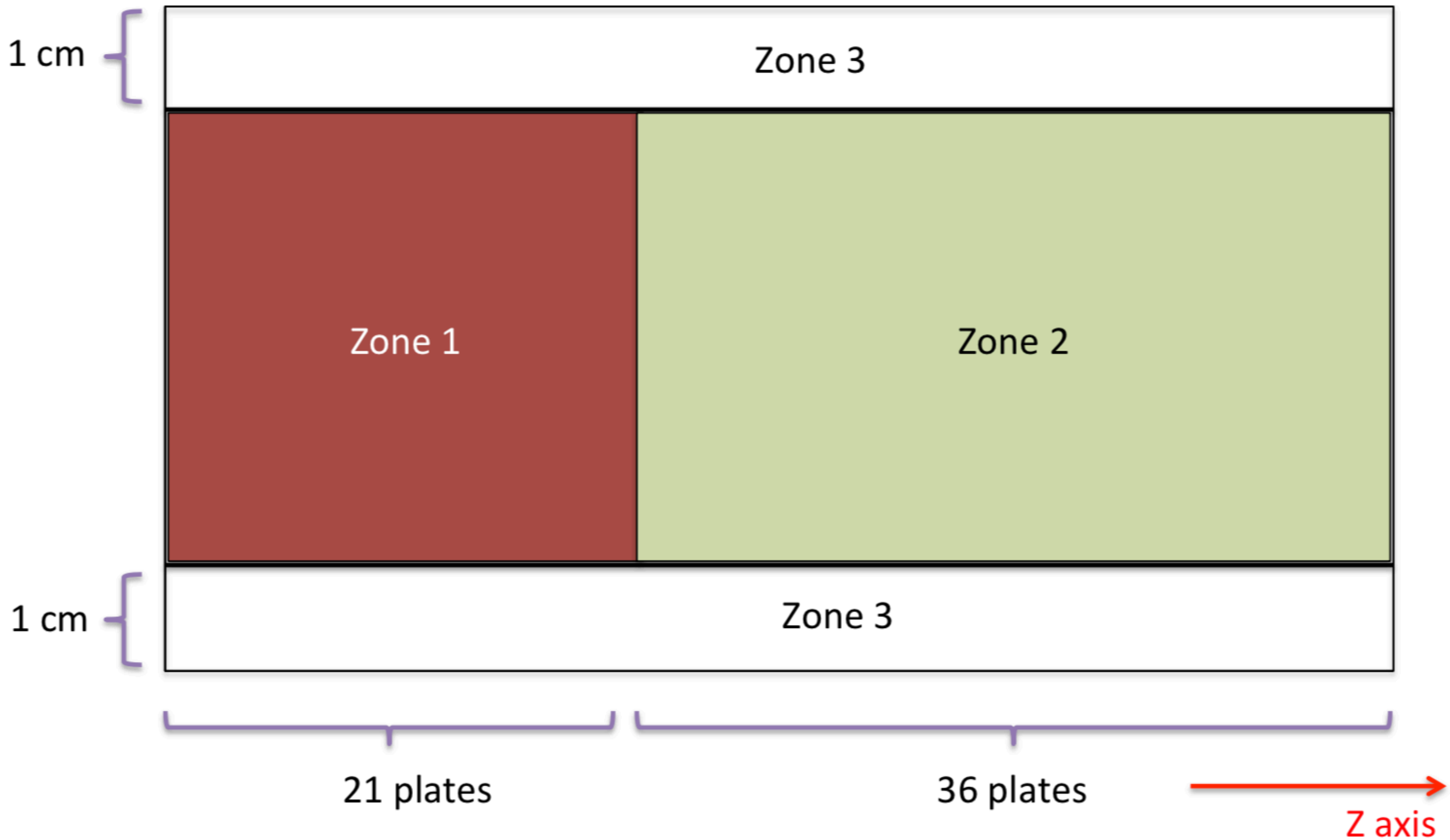

NUST MISIS, Russia, Moscow

Variables used in the analysis of Zone 1 events

A cone with opening angle 50 mrad is defined, starting from the decay point for the $\tau \to e$ decays, and from the primary vertex for ν_e events.

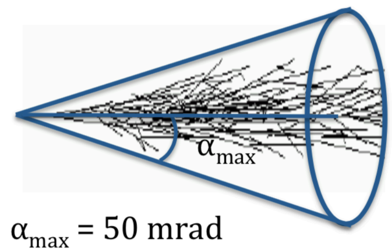

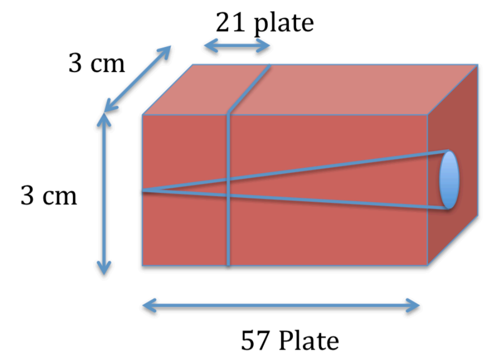

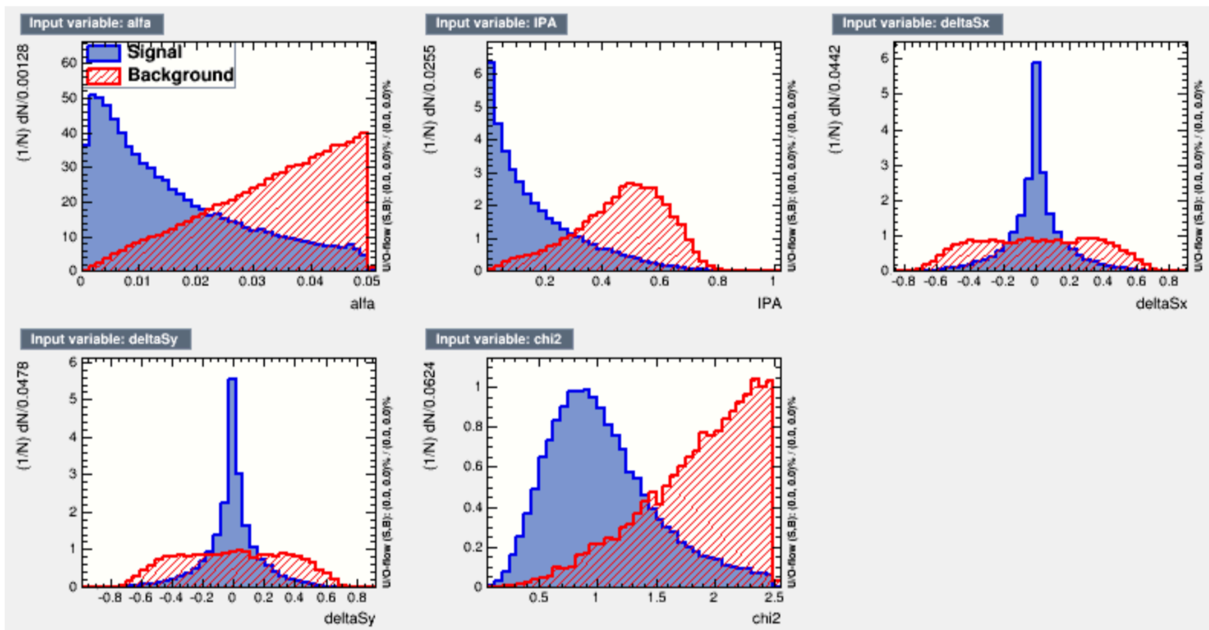

Energy Resolution

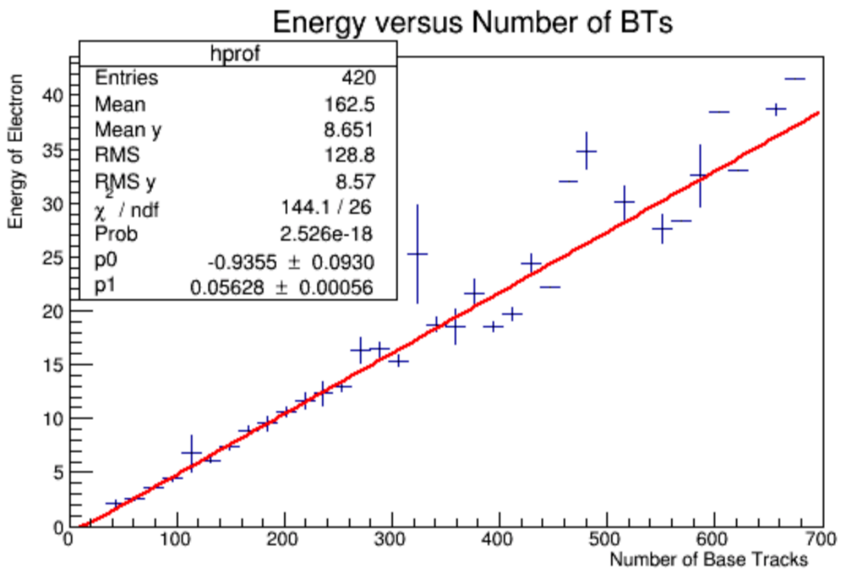

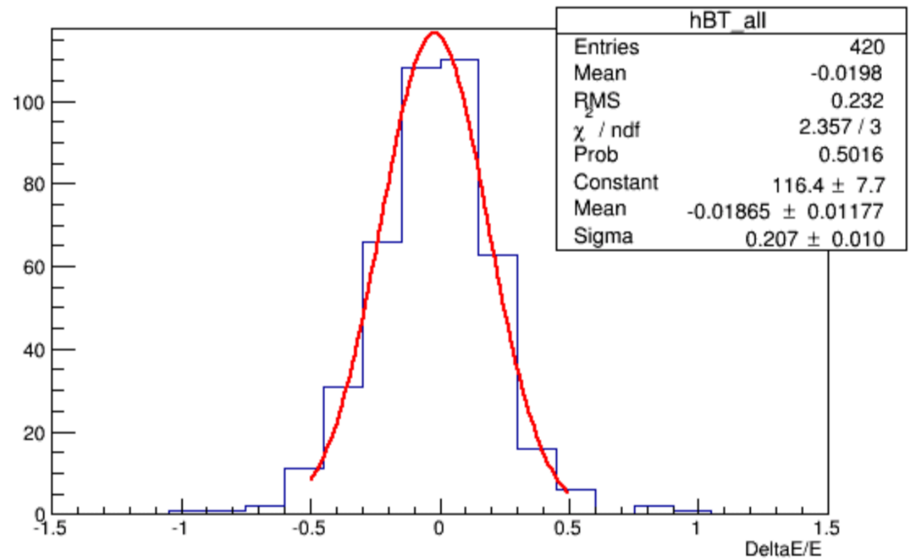

$$\frac{\Delta E}{E} = \frac{E_{true} - E_{meas}}{E_{true}} \qquad \sigma = 0.21$$

Average number of BTs per event (Signal) = 160

Average number of BTs per event (BG) = 17

FROM MGA TO NUST MISIS 100 YEARS 1918-2018 OPENING A NEW CENTURY

MISIS National University of Science and Technology

SHiP Search for Hidden Particles

LHCb

Analysis extended to the downstream brick

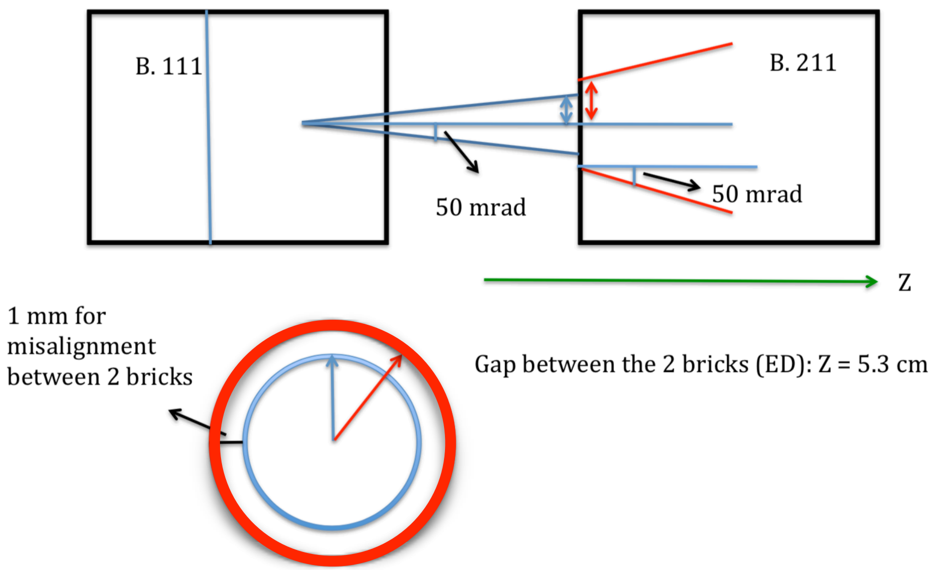

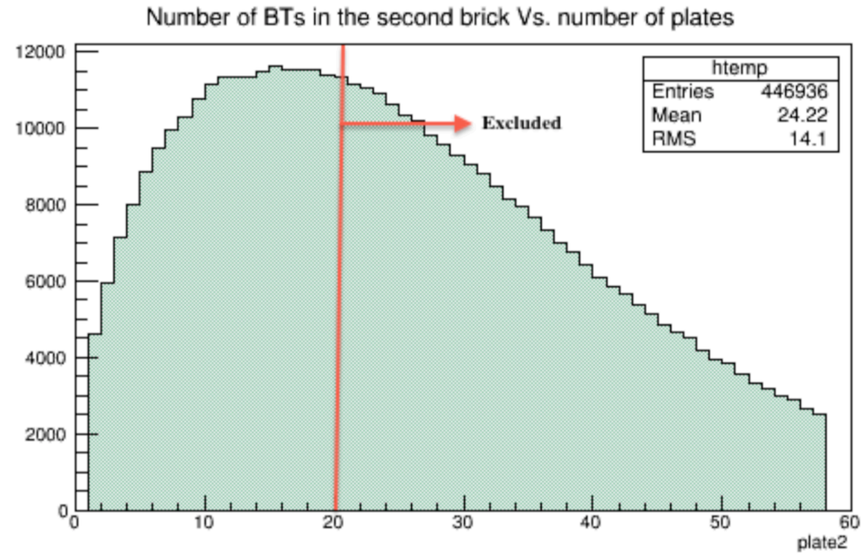

A volume of 20 films with a surface of 3x3 cm² each is scanned to estimate the background

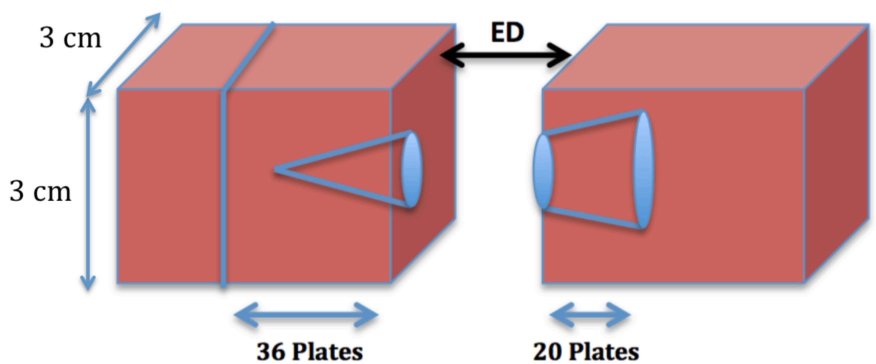

Resolution using the downstream brick

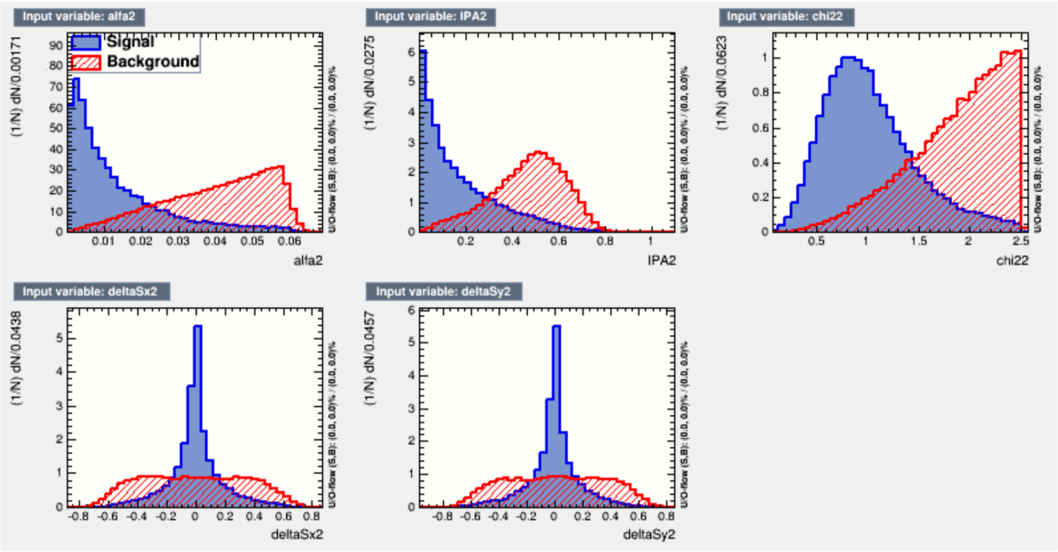

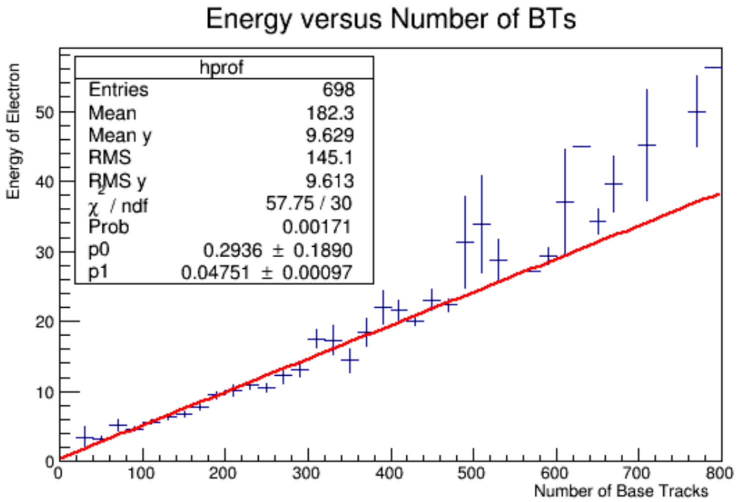

$$\frac{\Delta E}{E} = \frac{E_{true} - E_{meas}}{E_{true}} \qquad \sigma = 0.23$$

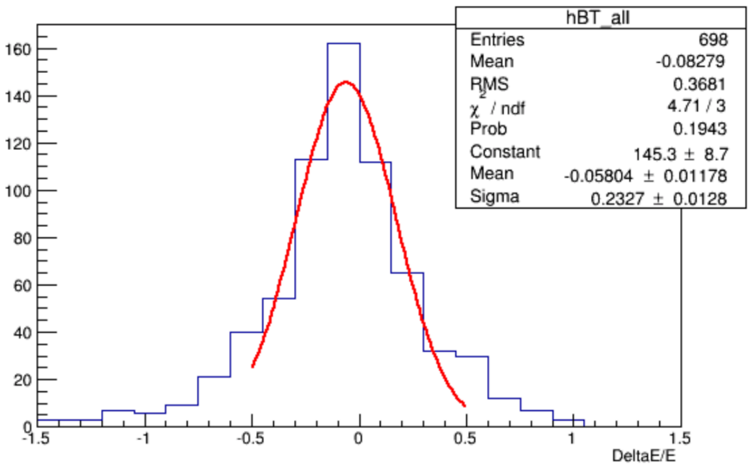

Average number of BTs per event (Signal) = 218

Average number of BTs per event (BG) = 18

NUST MISIS, Russia, Moscow

Hadronic Calorimetry

Hadron

$p^{\pm}, n, \pi^{\pm}, K^{\pm}, K^0$

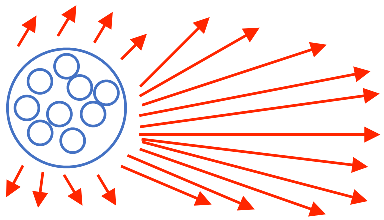

$\pi^{\pm}$

π^0

Strong Interaction

Approximate Energy Distribution

~50%	~20%	~30%
π^+, π^- π^0	Nuclear Excitation	Slow Nucleons
$\gamma\gamma$	5-30 MeV	
π^+, π^- π^+, π^-, π^0	p, n, γ	
$\gamma\gamma$		
Hadron Cascade		

$\pi^0 \rightarrow \gamma\gamma \rightarrow$ Electromagnetic Component

In Hadronic Cascades the longitudinal Shower is given by the Absorption Length λ_a

$$I \sim \exp^{-\frac{x}{\lambda_a}}$$

In typical Detector materials λ_a is much larger than X_0

$$\lambda \sim \frac{1}{9} \cdot 35 A^{\frac{1}{3}}$$

	ρ	X_0	λ
Fe	7,87	1.76cm	~17cm
Pb	11,35	0.56cm	~17cm

Energy Resolution:

- A large fraction of the Energy "disappears" into:
  - Binding Energy of the emitted Nucleons
  - $\pi \rightarrow \mu + \nu$ which are not absorbed
- π^0's decaying into $\gamma\gamma$ start EM Cascade ($\tau \sim 10^{-16}$s)

Energy resolution is worse than for EM Calorimeters

Hadron Calorimeters are Large because λ is large

Hadron Calorimeters are large and heavy because the hadronic interaction length λ, the "strong interaction equivalent" to the EM radiation length X_0, is large (5-10 times larger than X_0)

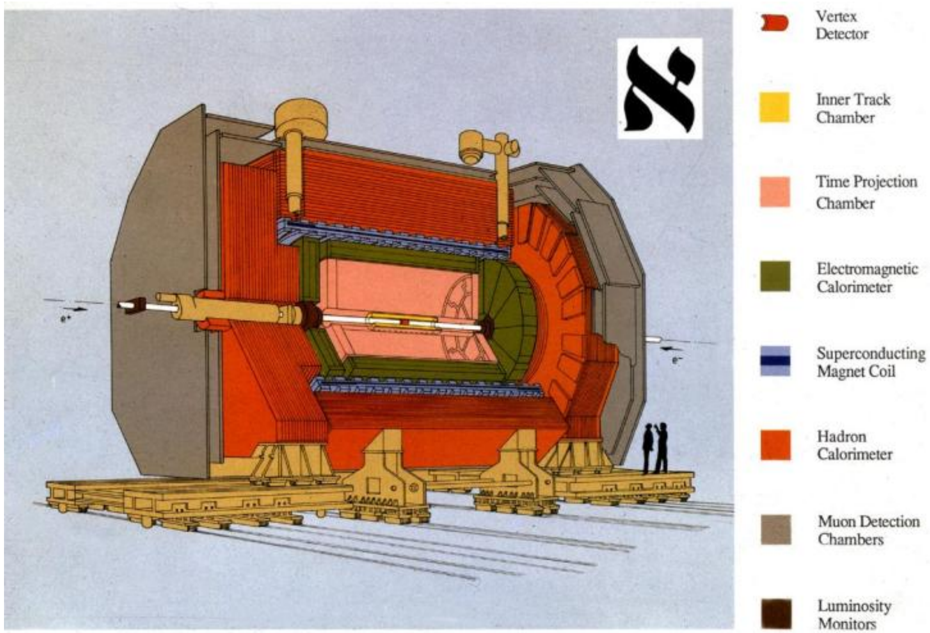

Fig. 1 - The ALEPH Detector

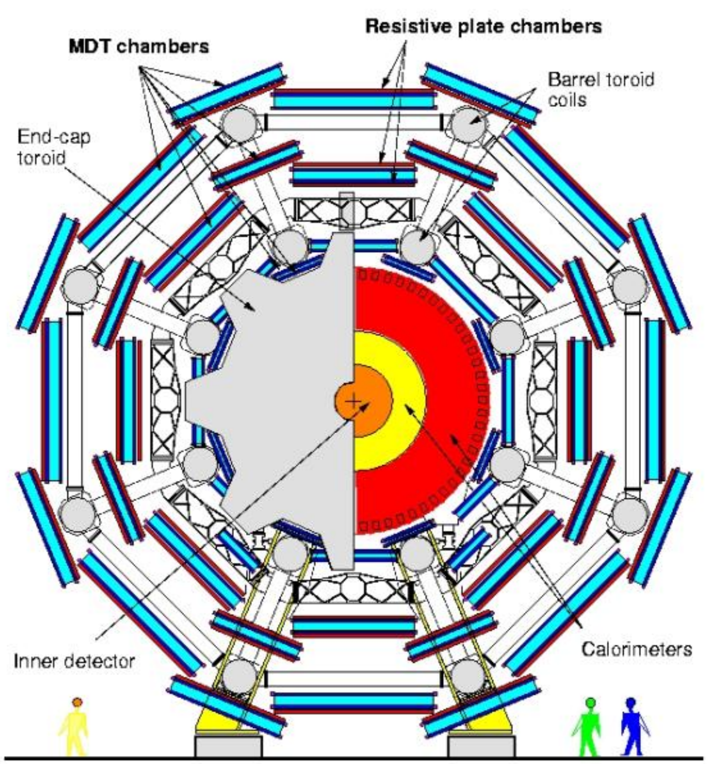

Hadron Calorimeters

By analogy with EM showers, the energy degradation of hadrons proceeds through an increasing number of (mostly) strong interactions with the calorimeter material.

However the complexity of the hadronic and nuclear processes produces a multitude of effects that determine the functioning and the performance of practical instruments, and make hadronic calorimeters more complicated instruments to optimize.

The hadronic interaction produces two classes of effects:

First, energetic secondary hadrons are produced. Their momenta are typically a sizable fraction of the primary hadron momentum i.e. at the GeV scale.

Second, in hadronic collisions with the material nuclei, a significant part of the primary energy is consumed in nuclear processes such as excitation, nucleon evaporation, spallation etc., resulting in particles with characteristic nuclear energies on the MeV scale.

Because part of the energy is therefore 'invisible', the resolution of hadron calorimeters is typically worse than in EM calorimeters 20-100%/Sqrt[E(GeV)] .

C.W. Fabjan and F. Gianotti, Rev. Mod. Phys., Vol. 75, N0. 4, October 2003

Hadron Calorimeters

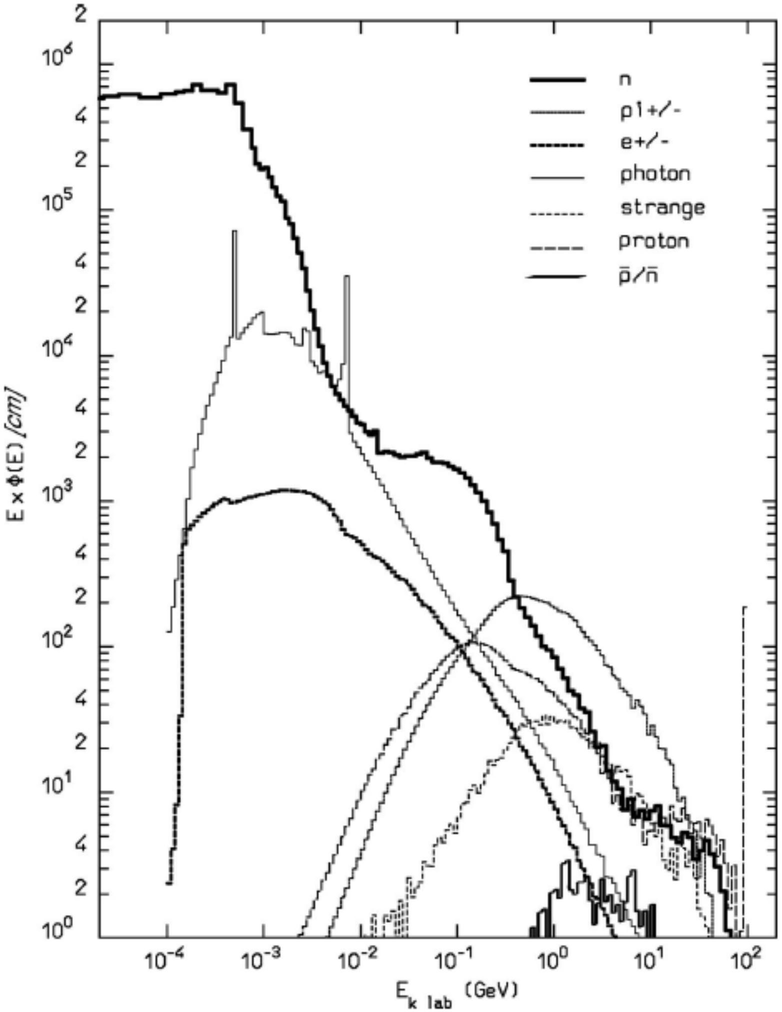

‘Deciphering this message becomes the story of hadronic calorimetry’

C.W. Fabjan and F. Gianotti, Rev. Mod. Phys., Vol. 75, N0. 4, October 2003

FIG. 19. Particle spectra produced in the hadronic cascade initiated by 100-GeV protons absorbed in lead. The energetic component is dominated by pions, whereas the soft spectrum is composed of photons and neutrons. The ordinate is in “lethargic” units and represents the particle track length, differential in log E. The integral of each curve gives the relative fluence of the particle. Fluka calculations (Ferrari, 2001).

Hadron Calorimeters

The signals from an electron or photon entering a hadronic calorimeter is typically larger than the signal from a hadron cascade because the hadronic interactions produce a fair fraction of invisible effects (excitations, neutrons ...)

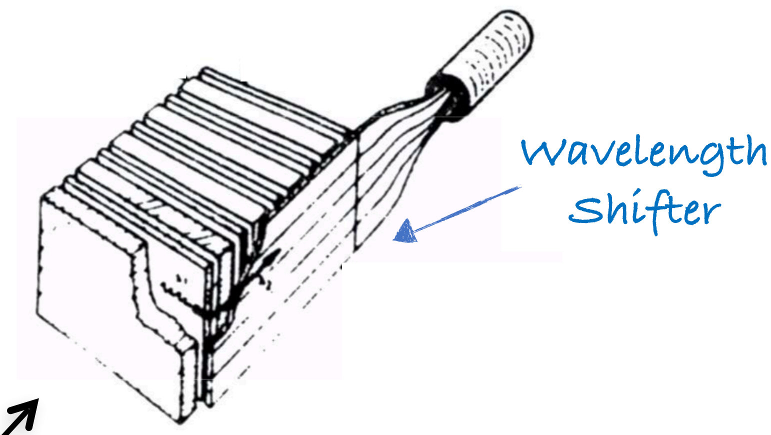

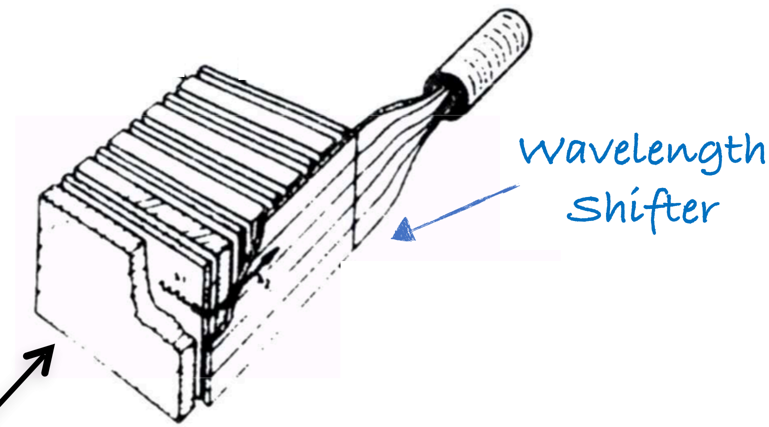

Pion 10GeV

Electron 10GeV

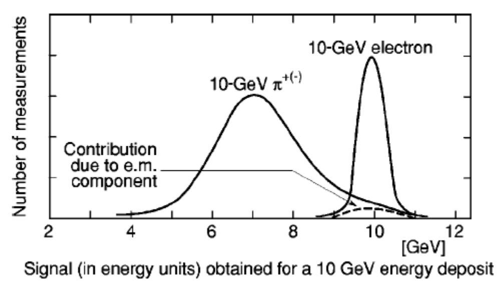

Hadron Calorimeters

Because a fair fraction of shower particles consists of π^0 which instantly decay into two photons, part of the hadronic cascade becomes an EM cascade – 'and never comes back'.

Because the EM cascade had a larger response than the Hadron cascade, the event/event fluctuation of produced π^0 particles causes a strong degradation of the resolution.

Is it possible to build a calorimeter that has the same response (signal) for a 10GeV electron and 10GeV hadron ? → compensating calorimeters.

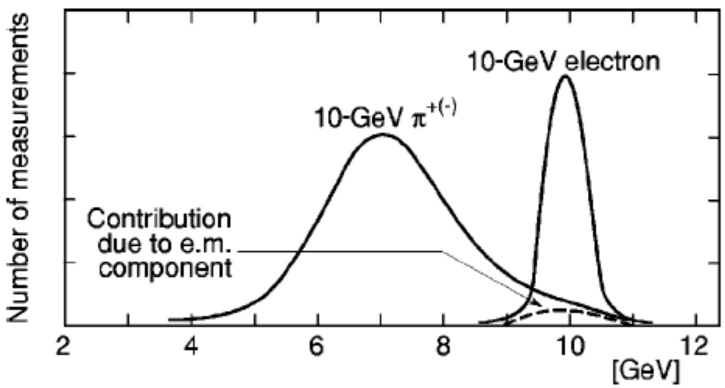

Signal (in energy units) obtained for a 10 GeV energy deposit

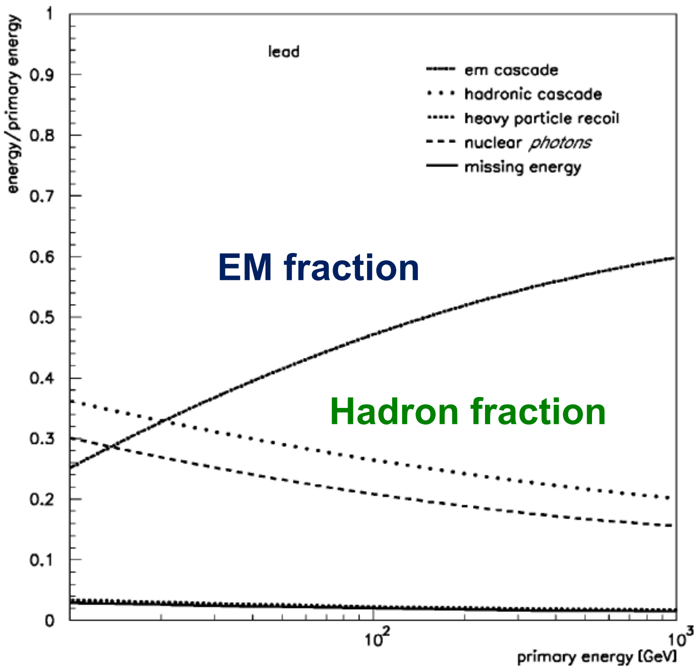

FIG. 21. Characteristic components of proton-initiated cascades in lead. With increasing primary energy the π^0 component increases (Ferrari, 2001).

Compensating Hadron Calorimeters

In a homogeneous calorimeter it is clearly not possible to have the same response for electrons and hadrons.

For sampling calorimeters the sampling frequency and thickness of active and passive layers can be tuned such that the signal for electrons and hadrons is indeed equal !

Using Uranium or Lead with scintillators, hadron calorimeters with excellent energy resolution and linearity have been built.

Energy resolution

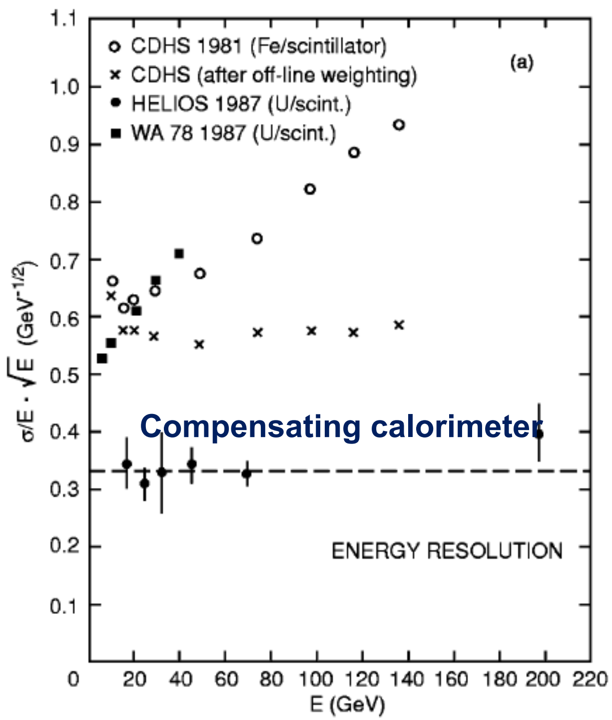

Linearity

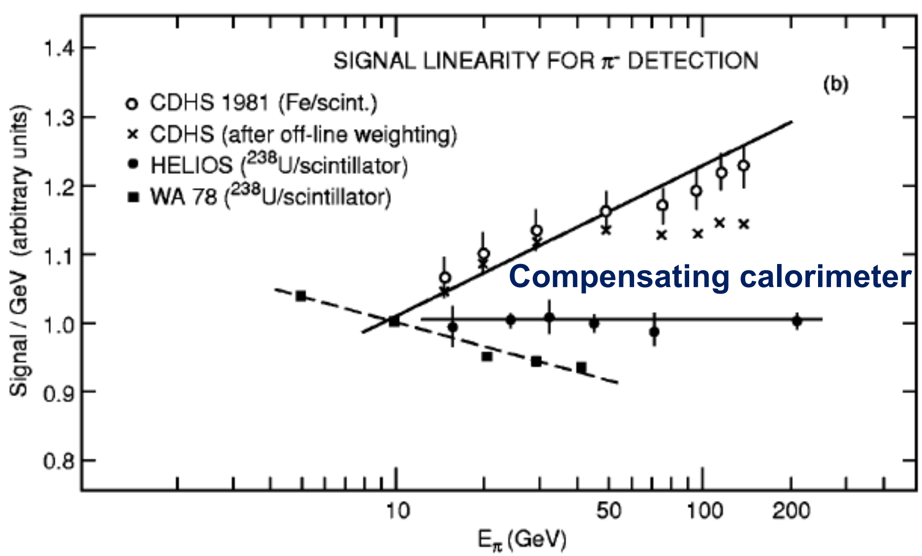

Compensating Hadron Calorimeters

Resolution and linearity of a hadron calorimeter is best if $e/h=1$. For all other values, the resolution in linearity is worse.

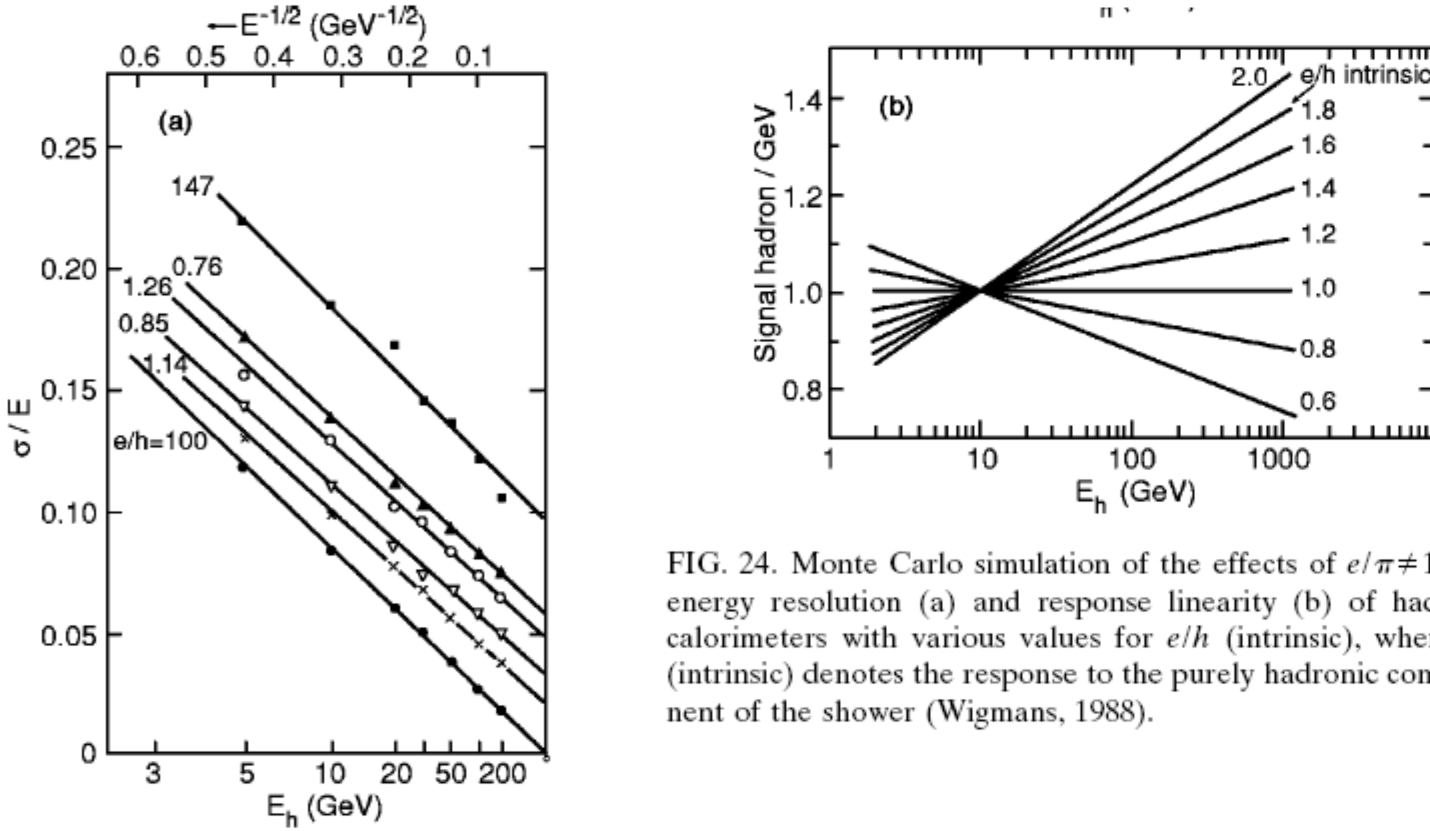

FIG. 24. Monte Carlo simulation of the effects of $e/\pi \neq 1$ on energy resolution (a) and response linearity (b) of hadron calorimeters with various values for e/h (intrinsic), where h (intrinsic) denotes the response to the purely hadronic component of the shower (Wigmans, 1988).

FROM MGA TO NUST MISIS 100 YEARS 1918-2018 OPENING A NEW CENTURY
MISIS National University of Science and Technology
SHiP Search for Hidden Particles
LHCb

Particle ID

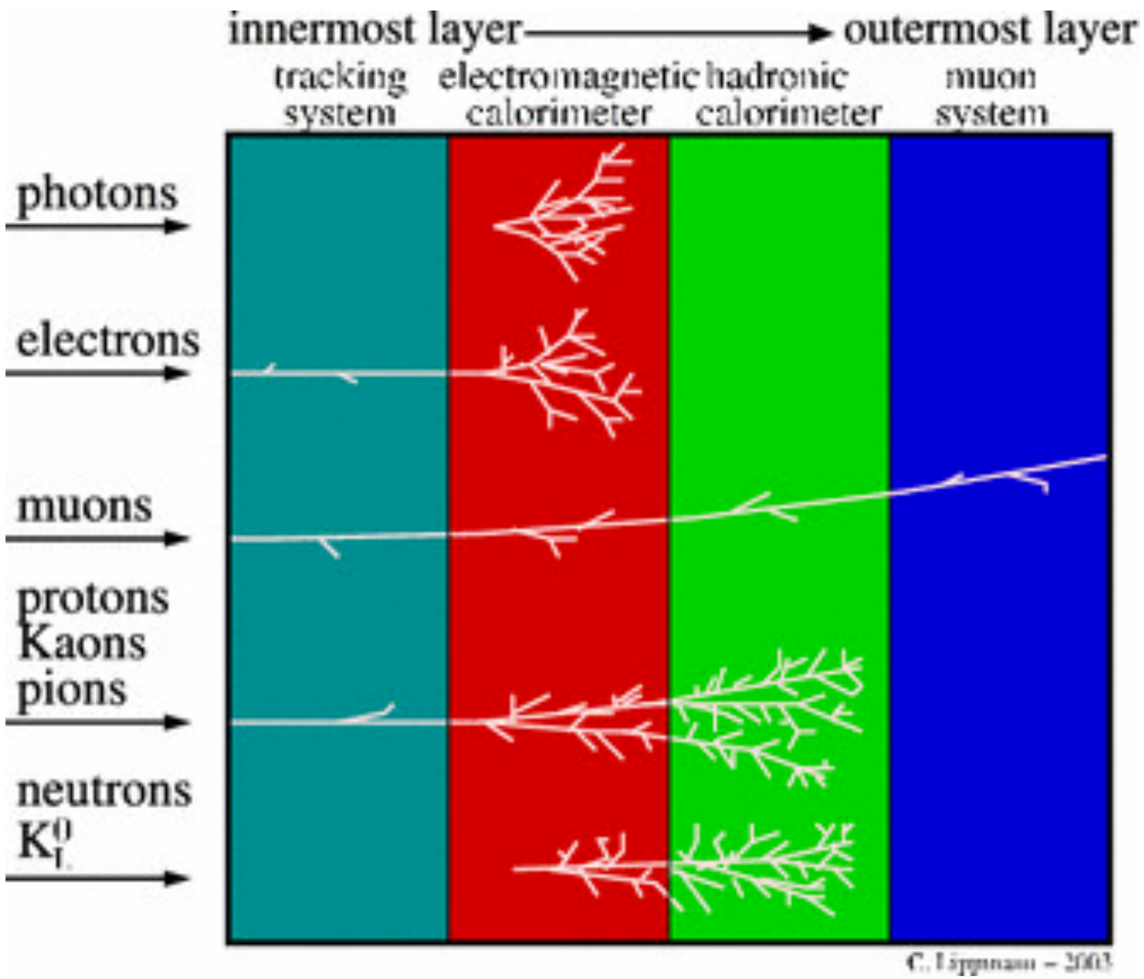
innermost layer
outermost layer
tracking system
electromagnetic calorimeter
hadronic calorimeter
muon system
photons
electrons
muons
protons
Kaons
pions
neutrons
K^0_L

Cherenkov Radiation

If the velocity of a charged particle is larger than the velocity of light in the medium v>c/n (n = Refractive index of material) it emits Cherenkov radiation of a characteristic angle of $\cos\theta_c = 1/n\beta$ ($\beta = v/c$)

Material	n-1	β threshold	γ threshold
solid sodium	3,22	0,24	1,029
lead glass	0,67	0,60	1,25
water	0,33	0,75	1,52
silica aerogel	0.025-0.075	0.93-0.976	2.7-4.6
air	2.99·10-4	0,9997	41,2
He	3.3·10-5	0,99997	123

$$\frac{dN}{dx} \sim 2\pi\alpha Z_1^2 \left(1 - \frac{1}{\beta^2 n^2}\right) \frac{\lambda_2 - \lambda_1}{\lambda_2 \cdot \lambda_1}$$

Numbers of emitted Photons\length with λ between λ_1 and λ_2 with λ_1=400 nm, λ_2=700 nm

$$\frac{dN}{dx} = 490 \left(1 - \frac{1}{\beta^2 n^2}\right) \left[\frac{1}{cm}\right]$$

FROM MGA TO NUST MISIS 100 YEARS 1918-2018 OPENING A NEW CENTURY | MISIS National University of Science and Technology | SHiP Search for Hidden Particles | LHCb

Ring Imaging Cherenkov Detector

$$\cos\theta = \frac{1}{n\beta}$$

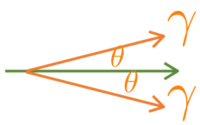

UV Photon

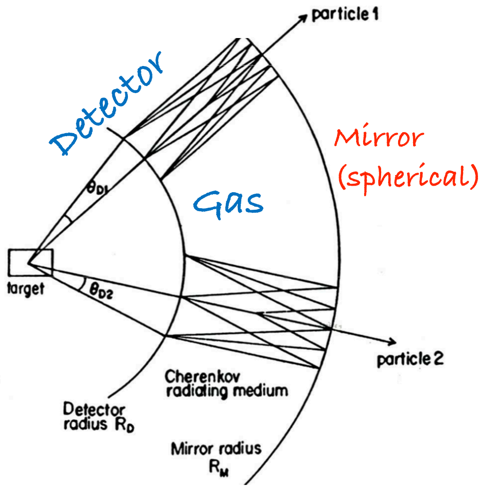

200 GeV/c K, π

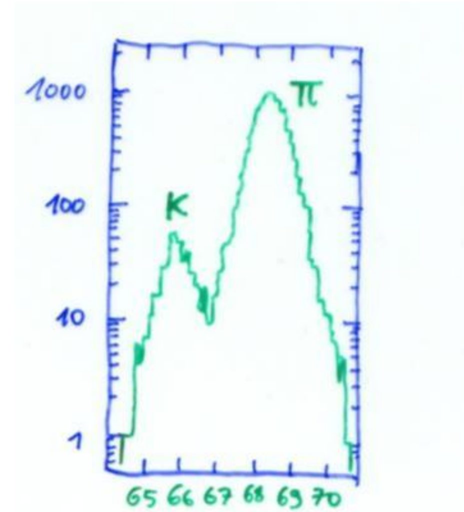

Ring Radius [mm]

Resolution:

$$\frac{\Delta\gamma}{\gamma} = \gamma^2\beta^2 n\Delta\theta\frac{1}{\sqrt{N_0 L}} \qquad \left(\gamma = \frac{1}{\sqrt{1-\beta^2}}\right)$$

Angle measurement accuracy

Photon Statistics

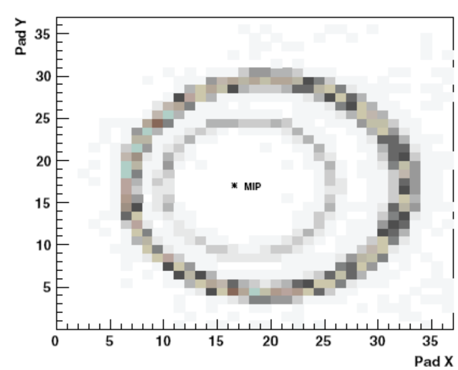

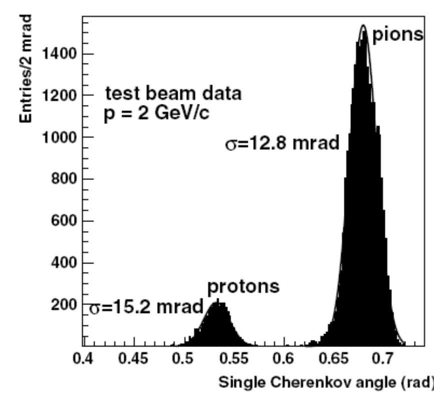

FROM MGA TO NUST MISIS 100 YEARS 1918-2018 OPENING A NEW CENTURY
MISIS National University of Science and Technology
SHiP Search for Hidden Particles
LHCb

Measuring the neutrino energy: the OPERA experiment as an example

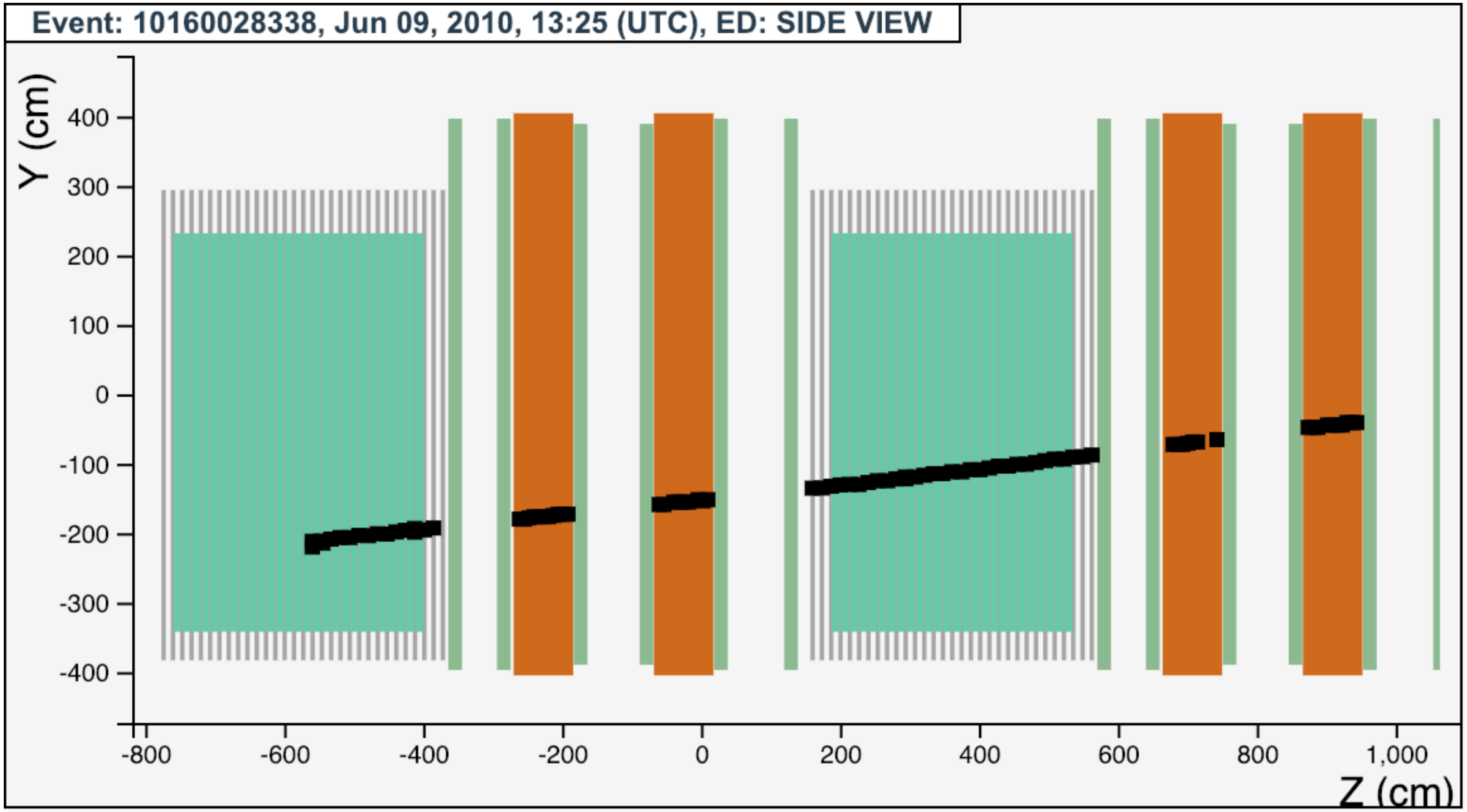

Measuring neutrino energy in OPERA

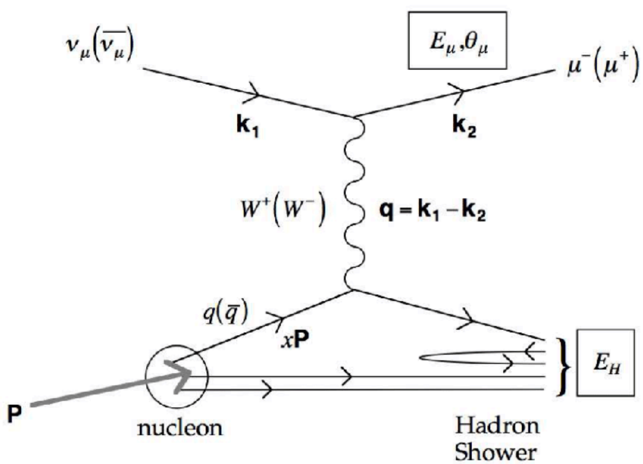

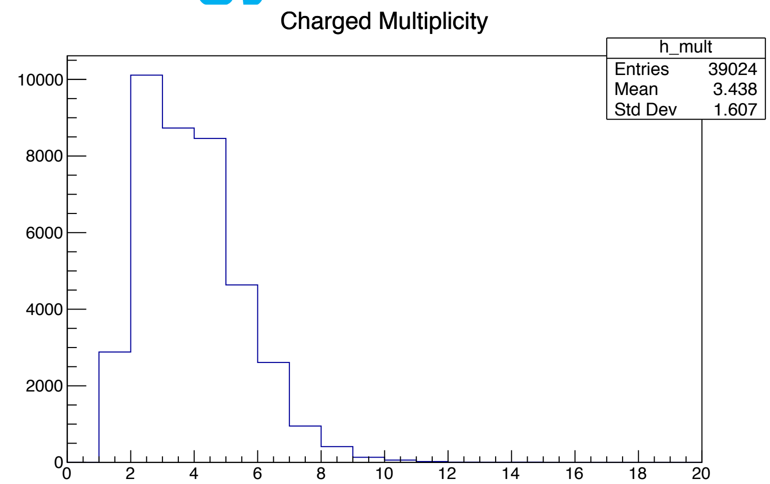

ν_μCC events with at least one reconstructed muon

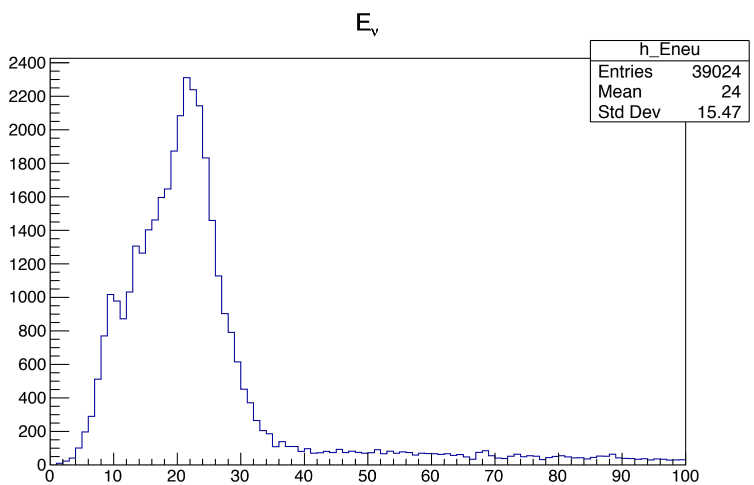

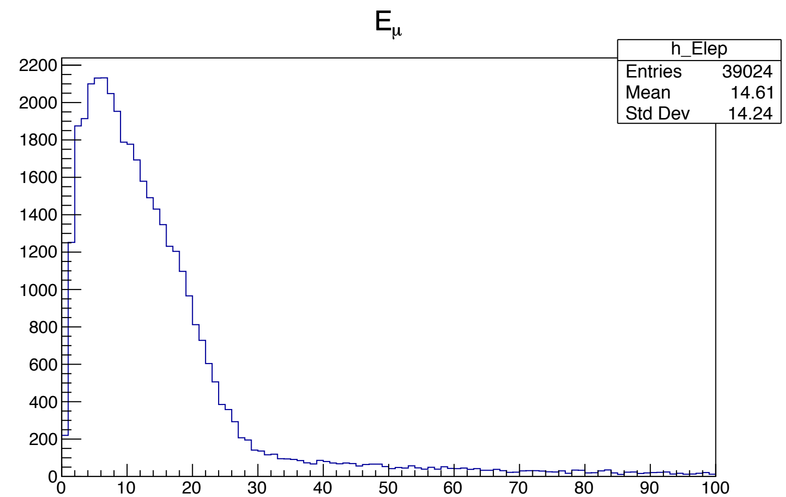

FROM MGA TO NUST MISIS 100 YEARS 1918-2018 OPENING A NEW CENTURY
MISIS National University of Science and Technology
SHiP Search for Hidden Particles
LHCb

NUST MISIS, Russia, Moscow

Measuring neutrino energy in OPERA

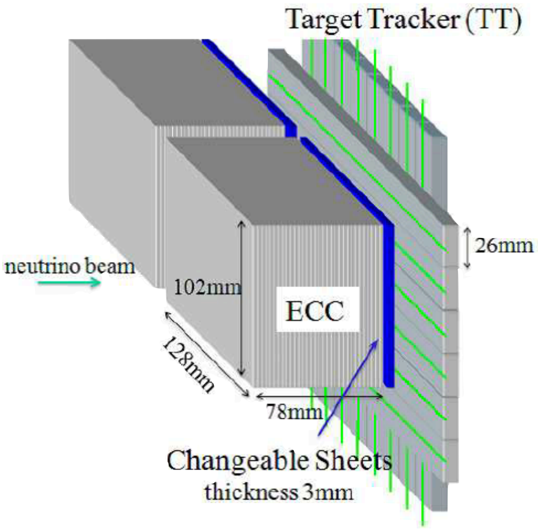

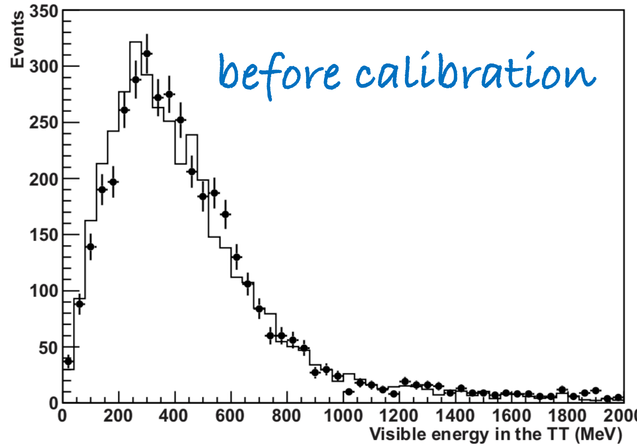

Energy deposit (before calibration) in the TT for events with at least one reconstructed muon.
Dots with error bars correspond to data and solid lines to MC.
MC distributions are normalized to data.

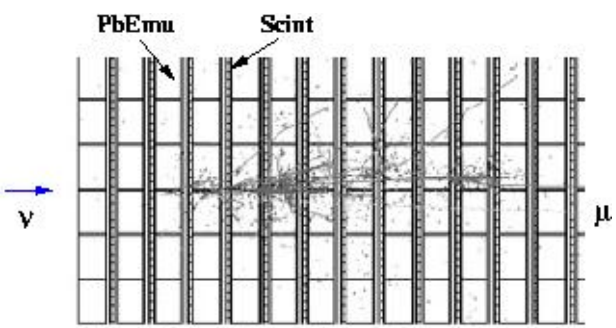

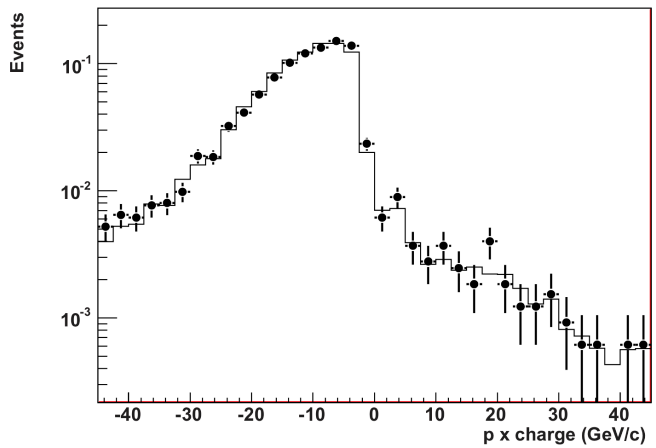

Muon charge comparison (momentum × charge): data (black dots with error bars) and MC (solid line) are normalized to 1.

Measuring neutrino energy in OPERA

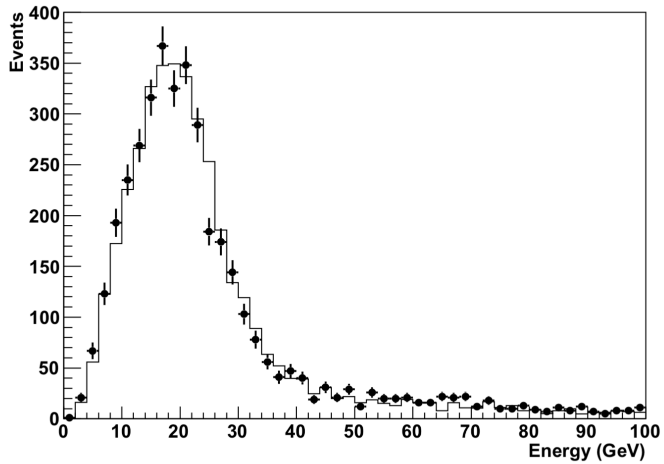

Total reconstructed energy for events with at least one identified muon for data (dots with error bars) and MC (solid line). The MC distribution is normalized to data.

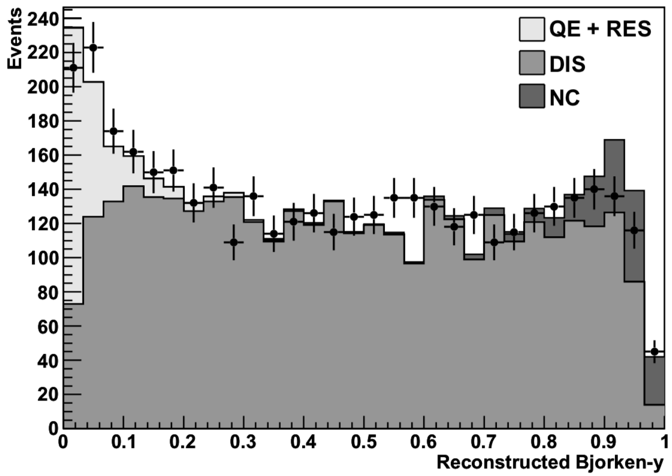

$$y_B = 1 - \frac{E_\mu}{E_{\nu_\mu}} = \frac{E_{had}}{E_\mu + E_{had}}$$

Bjorken-y variable reconstructed in data (dots with error bars) and MC (shaded areas) for all the events with at least one muon.
The MC distributions are normalized to data.

Measuring energy with a SHiP prototype

- Prototype of the SHiP Scattering and Neutrino detector to take data at the LHC in Run3
- Combining electromagnetic (Emulsion + SciFi) and hadronic calorimeter (SciFi +

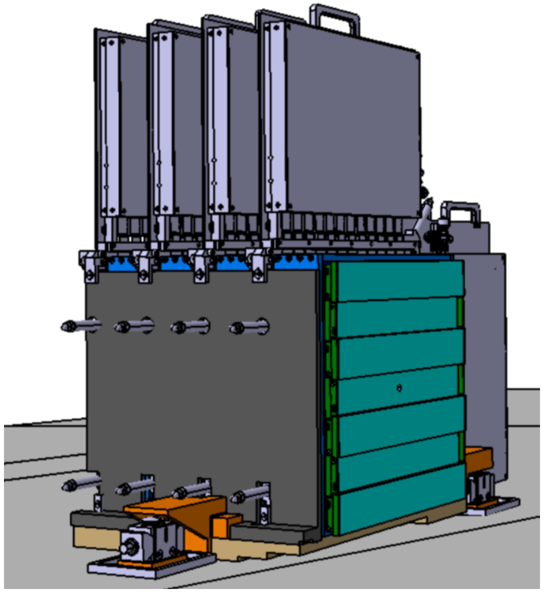

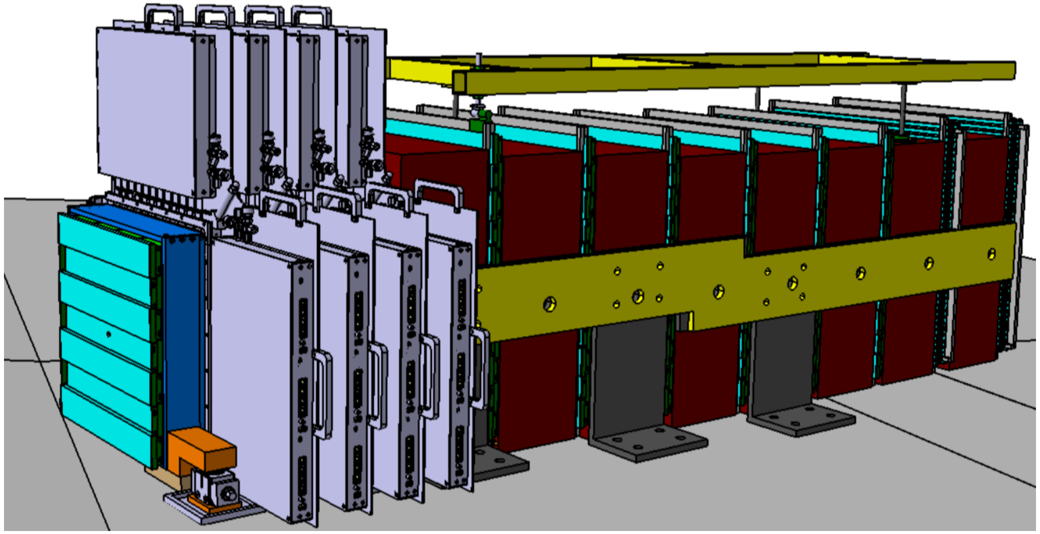

$$\sigma(E_{had}) = (18.8 \pm 0.2)\%$$

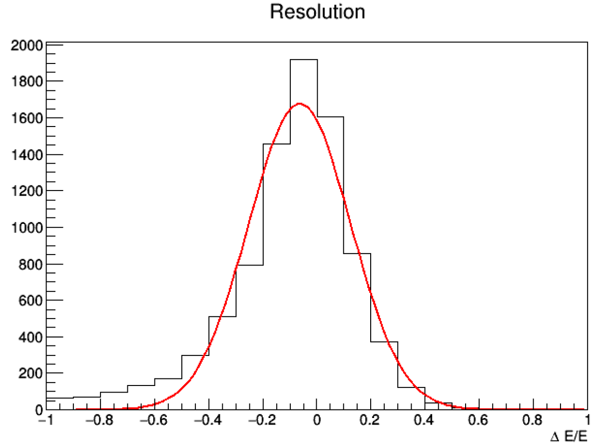

Conclusion

The story of modern calorimetry is a textbook example of physics research driving the development of an experimental method.

The long quest for precision electron and photon spectroscopy explains the remarkable progress in new instrumentation techniques, for both sampling and homogeneous calorimeters.

The study of jets of particles as the macroscopic manifestation of quarks has driven the work on hadronic calorimeters.

Calorimeters largely used also in neutrino physics